Poisson Multi-Bernoulli Mixture Conjugate Prior for Multiple Extended Target Filtering

KARL GRANSTRÖM, Member, IEEE
Chalmers University of Technology, Gothenburg, Sweden

MARYAM FATEMI
Zenuity, Gothenburg, Sweden

LENNART SVENSSON
Chalmers University of Technology, Gothenburg, Sweden

This paper presents a Poisson multi-Bernoulli mixture (PMBM) conjugate prior for multiple extended object filtering. A Poisson point process is used to describe the existence of yet undetected targets, while a multi-Bernoulli mixture describes the distribution of the targets that have been detected. The prediction and update equations are presented for the standard transition density and measurement likelihood. Both the prediction and the update preserve the PMBM form of the density, and in this sense, the PMBM density is a conjugate prior. However, the unknown data associations lead to an intractably large number of terms in the PMBM density, and approximations are necessary for tractability. A gamma Gaussian inverse Wishart implementation is presented, along with methods to handle the data association problem. A simulation study shows that the extended target PMBM filter performs well in comparison to the extended target δ-generalized labelled multi-Bernoulli and LMB filters. An experiment with Lidar data illustrates the benefit of tracking both detected and undetected targets.

Manuscript received March 31, 2017; revised June 19, 2018, November 21, 2018, and March 28, 2019; released for publication April 6, 2019. Date of publication June 4, 2019; date of current version February 7, 2020.

DOI. No. 10.1109/TAES.2019.2920220

Refereeing of this contribution was handled by S. Maskell.

Authors' addresses: K. Granström and L. Svensson are with the Department of Signals and Systems, Chalmers University of Technology, Gothenburg 41296, Sweden, E-mail: (karl.granstrom@chalmers.se; lennart.svensson@chalmers.se); M. Fatemi is with the Zenuity, Gothenburg 41756, Sweden, E-mail: (maryam.fatemi@zenuity.com). *(Corresponding author: Karl Granström.)*

I. INTRODUCTION

Multiple target tracking (MTT) is the processing of sets of measurements obtained from multiple sources in order to maintain estimates of the targets' current states.[1] Solving the MTT problem is complicated by the fact that—in addition to noise, missed detections and clutter—the number of targets is unknown and time-varying. Point target MTT is defined as tracking targets that give rise to at most one measurement per target at each time step, and extended target MTT is defined as tracking targets that potentially give rise to more than one measurement at each time step, where the set of measurements are spatially distributed around the extended target.

The focus of this paper is on extended targets. A target may give rise to more than one measurement if the resolution of the sensor, the size of the target, and the distance between target and sensor, are such that multiple resolution cells of the sensor are occupied by a single target. Examples of such scenarios include vehicle tracking using automotive radars, tracking of ships with marine radar stations, and person tracking using laser range sensors. An introduction to extended target tracking and a comprehensive overview of the literature is given in [1].

A common extended target measurement model is the inhomogeneous Poisson point process (PPP), proposed in [2]. At each time step, a Poisson distributed random number of measurements are generated, distributed around the target. For tracking multiple extended targets, random finite sets (RFSs) can be used to model the problem. RFSs and Finite set statistics [3], [4] are a theoretically elegant and appealing approach to the MTT problem where targets and measurements are modeled as random sets. The PPP extended target model [2] has been integrated into several computationally feasible RFS-based filters, e.g., [5]–[10].

In Bayesian statistics, the concepts of *conjugacy* and *conjugate prior*, first introduced by Raiffa and Schlaifer [11], are important. Conjugacy in the context of MTT means that *"if we start with the proposed conjugate initial prior, then all subsequent predicted and posterior distributions have the same form as the initial prior"* [12, p. 3460]. MTT conjugate priors are of great interest as they provide families of distributions that are suitable to work with when we seek accurate approximations to the posterior distributions.

Two different kinds of MTT conjugate priors can be found in the literature: one based on labelled multi-Bernoulli (MB) RFSs, called δ-generalized labelled multi-Bernoulli (δ-GLMB) [12]; and another based on Poisson MB RFSs, called Poisson multi-Bernoulli mixture (PMBM) [13]. The PMBM conjugate prior allows an elegant separation of the set of targets into two disjoint subsets: targets that have been detected, and targets that are unknown, i.e., that have not yet been detected. For the δ-GLMB

[1]In MTT, a multitarget *tracker* produces estimates of target trajectories (state sequences), while a multitarget *filter* produces estimates of the current set of targets. In this paper, we focus on filtering, whereas forming target trajectories is outside the scope of the paper.

multiobject density, conjugacy has been shown for both point targets [12] and extended targets [9]; for the PMBM multiobject density, conjugacy has only been shown for point targets [13].

The relation between the two point target conjugate priors are explored in [14], where it is shown that the PMBM density has a more efficient structure than the δ-GLMB density, with fewer hypotheses. A performance comparison of different implementations of point target filters based on MTT conjugate priors was presented in [15], and it showed that the filters based on the PMBM conjugate prior in general compare well to the filters based on the δ-GLMB conjugate prior, in terms of the tracking performance[2] and computational cost. It is, therefore, of interest to prove conjugacy for the PMBM multiobject density also for the standard extended target likelihood [2], and to implement a PMBM filter for extended targets and compare its performance to the δ-GLMB filter for extended targets.

In this paper, we derive a PMBM MTT conjugate prior for the PPP measurement model [2] and the standard multitarget motion model, see, e.g., [3, p. 314]. A preliminary version of this paper was presented in [17]. This paper is a significant extension of that work, and contains the following contributions.

1) In Section IV, we derive, for the PPP extended target likelihood, the conjugate update for the PMBM density, and we review the conjugate prediction for the PMBM density, which was presented in [13].
2) In Section V, we analyse the complexity of the PMBM filter, discuss how the data association problem can be handled, and analyze the approximation error that is incurred by approximating the data association. In Section V-C, we propose a merging algorithm that can be used to reduce the number of components in an MB mixture (MBM).
3) In Section VI, we present a computationally feasible implementation of the PMBM filter, based on gamma Gaussian inverse Wishart (GGIW) single target models.
4) In Section VII, we present a simulation study, where the GGIW-PMBM filter is compared to state-of-the-art algorithms, and we present an experiment, in which the benefits of modeling the targets that have not yet been detected is highlighted.

Problem formulation and modeling are presented in Sections II and III, respectively. This paper is concluded in Section VIII.

II. PROBLEM FORMULATION

The set of targets at time step k is denoted $\mathbf{X}_k$, and is modeled as an RFS, meaning that the target set cardinality $|\mathbf{X}_k|$ is a time-varying discrete random variable, and each target state is a random variable. The target state models both kinematic properties (position, velocity, turn-rate, orientation, etc) and target extent (shape and size). The set of measurements at time step k is an RFS denoted $\mathbf{Z}_k$. There are two types of measurements: clutter measurements and target originated measurements, and the measurement origin is assumed unknown. Furthermore, $\mathbf{Z}^k$ denotes all measurement sets $\mathbf{Z}_t$ from time $t = 0$ up to, and including, time $t = k$.

The multiobject posterior density at time k, given all measurement sets up to and including time step k, is denoted $f_{k|k}(\mathbf{X}_k|\mathbf{Z}^k)$. The multitarget Bayes filter propagates in time the multitarget set density $f_{k-1|k-1}(\mathbf{X}_{k-1}|\mathbf{Z}^{k-1})$ using the Chapman–Kolmogorov prediction

$$f_{k|k-1}(\mathbf{X}_k|\mathbf{Z}^{k-1}) = \int f_{k,k-1}(\mathbf{X}_k|\mathbf{X}_{k-1}) f_{k-1|k-1}(\mathbf{X}_{k-1}|\mathbf{Z}^{k-1}) \delta\mathbf{X}_{k-1} \quad (1a)$$

and then updates the density using the Bayes update

$$f_{k|k}(\mathbf{X}_k|\mathbf{Z}^k) = \frac{f_k(\mathbf{Z}_k|\mathbf{X}_k) f_{k|k-1}(\mathbf{X}_k|\mathbf{Z}^{k-1})}{\int f_k(\mathbf{Z}_k|\mathbf{X}_k) f_{k|k-1}(\mathbf{X}_k|\mathbf{Z}^{k-1}) \delta\mathbf{X}_k} \quad (1b)$$

where $f_{k+1,k}(\mathbf{X}_{k+1}|\mathbf{X}_k)$ is the multiobject transition density, $f_k(\mathbf{Z}_k|\mathbf{X}_k)$ is the multitarget measurement set density, and the integrals are set-integrals, defined in [3, Sec. 11.3.3]. In this paper, we model the measurement set density $f_k(\mathbf{Z}_k|\mathbf{X}_k)$ using the standard PPP extended target measurement model [2] and a standard PPP clutter model. The multiobject transition density $f_{k+1,k}(\mathbf{X}_{k+1}|\mathbf{X}_k)$ is modeled by a standard multiobject Markov density with PPP birth.

Among RFS-based filters, there are two main filter types that implement the Bayes recursion (1) for the multiobject density. The first is based on moment approximations, e.g., the PHD filter and the CPHD filter. The second is based on parameterized density representations, e.g., the GLMB filter and the PMBM filter.

Following are the main objectives of this paper.

1) To show that the PMBM representation of $f_{k|k}(\mathbf{X}_k|\mathbf{Z}^k)$ is an MTT conjugate prior for the standard extended target tracking models by deriving the corresponding prediction and update.
2) To show how this PMBM filter can be implemented in a computationally tractable way.
3) To evaluate the performance of the implementation and compare to state-of-the-art algorithms.

III. MODELING

An introduction to RFSs is given in, e.g., [3], and an introduction to extended object modeling is given in, e.g., [1]. This section first presents a review of random set theory; specifically, the PPP and the Bernoulli process. The standard extended target measurement and motion models are then presented. Notation is given in Table I.

A. Review of Random Set Modeling

1) *PPP:* A PPP is a type of RFS whose cardinality is Poisson distributed, and all elements (e.g., target states) are independent and identically distributed. A PPP can be

[2]The tracking performance is measured by the localisation error, number of false targets (FT), and number of missed targets (MT), see, e.g., [16, Sec. 13.6].

TABLE I
Notation

- Minor non-bold letters, e.g., α, β, γ, denote scalars, minor bold letters, e.g., $\mathbf{x}, \mathbf{z}, \boldsymbol{\xi}$, denote vectors, capital non-bold letters, e.g., X, H, F denote matrices, and capital bold letters, e.g., $\mathbf{X}, \mathbf{Z}, \mathbf{C}$, denote sets.
- $|V|$: determinant of matrix V.
- $|\mathbf{X}|$: cardinality of set $\mathbf{X}$, i.e., number of elements in set $\mathbf{X}$.
- $\mathbf{I}_m$: identity matrix of size $m \times m$.
- $\langle a; b \rangle = \int a(x)b(x)\mathrm{d}x$: inner product of $a(x)$ and $b(x)$
- $h^{\mathbf{X}} = \prod_{\mathbf{x}\in\mathbf{X}} h(\mathbf{x})$, where $h^{\emptyset} = 1$ by definition.
- $\sum_{\uplus_{i\in\mathbb{I}}\mathbf{X}^i=\mathbf{X}}$: a sum over all (possibly empty) subsets $\mathbf{X}^i$, $i \in \mathbb{I}$, that are mutually disjoint, and whose union is $\mathbf{X}$, see [3, Sec. 11.5.3].
- $\binom{a}{b} = \frac{a!}{b!(a-b)!}$: Binomial coefficient
- $\left\{ {a \atop b} \right\} = \frac{1}{b!}\sum_{k=0}^{b}(-1)^{b-k}\binom{b}{k}k^a$: Stirling number of the second kind
- $B(n)$: Bell number of n:th order

parameterized by an intensity function $D(\mathbf{x})$, defined on single target state space. The intensity function can be broken down into two parts $D(\mathbf{x}) = \mu f(\mathbf{x})$: the scalar Poisson rate $\mu > 0$ and the spatial distribution $f(\mathbf{x})$. One important property of the intensity is that $\int_{\mathbf{x}\in S} D(\mathbf{x})\mathrm{d}\mathbf{x}$ is the expected number of set members in S. This can be interpreted to mean that in parts of the state space with high/low intensity $D(\mathbf{x})$, there is a high/low chance that set members are located. The PPP density is

$$f(\mathbf{X}) = e^{-\langle D;1\rangle}\prod_{\mathbf{x}\in\mathbf{X}} D(\mathbf{x}) = e^{-\mu}\prod_{\mathbf{x}\in\mathbf{X}} \mu f(\mathbf{x}). \tag{2}$$

In this paper, PPPs are used to model clutter measurements, extended target measurements, target birth, and undetected targets.

2) *Bernoulli Process:* A Bernoulli RFS $\mathbf{X}$ is a type of RFS that is empty with probability $1 - r$ or, with probability r, contains a single element with probability density function $f(\mathbf{x})$. The cardinality is, therefore, Bernoulli distributed with parameter $r \in [0, 1]$. The Bernoulli density is

$$f(\mathbf{X}) = \begin{cases} 1-r & \mathbf{X} = \emptyset \\ rf(\mathbf{x}) & \mathbf{X} = \{\mathbf{x}\} \\ 0 & |\mathbf{X}| \geq 2 \end{cases}. \tag{3}$$

In MTT, a Bernoulli RFS is a natural representation of a single target, as it captures both the uncertainty regarding the target's existence (via the parameter r), as well as the uncertainty regarding the target's state $\mathbf{x}$ (via the density $f(\mathbf{x})$).

For an index set $\mathbb{I}$, an MB RFS $\mathbf{X}$ is the union of a fixed number of independent Bernoulli RFSs $\mathbf{X}^i$, $i \in \mathbb{I}$, where $\mathbf{X}^i \cap \mathbf{X}^j = \emptyset$ for all i, $j \in \mathbb{I}$, and $\cup_{i\in\mathbb{I}}\mathbf{X}^i = \mathbf{X}$. The MB density for a set $\mathbf{X}$ can be expressed as

$$f(\mathbf{X}) = \begin{cases} \sum_{\uplus_{i\in\mathbb{I}}\mathbf{X}^i=\mathbf{X}} \prod_{i\in\mathbb{I}} f^i(\mathbf{X}^i) & \text{if} \quad |\mathbf{X}| \leq |\mathbb{I}| \\ 0 & \text{if} \quad |\mathbf{X}| > |\mathbb{I}| \end{cases} \tag{4}$$

where the notation $\uplus$ is defined in Table I. The MB distribution is defined entirely by the parameters $\{r^i, f^i\}_{i\in\mathbb{I}}$ of the involved Bernoulli RFSs.

Finally, an MBM density is an RFS density that is a normalized, weighted sum of MB densities. In MTT, the weights typically correspond to the probability of different data association sequences. An MBM is defined entirely by the set of parameters $\{(\mathcal{W}^j, \{(r^{j,i}, f^{j,i})\}_{i\in\mathbb{I}^j})\}_{j\in\mathbb{J}}$, where $\mathbb{J}$ is an index set for the MBs in the MBM (also called components of the MBM), $\mathbb{I}^j$ is an index set for the Bernoullis in the jth MB, and $\mathcal{W}^j$ is the probability of the jth MB.

B. Standard Extended Target Measurement Model

The set of measurements $\mathbf{Z}_k$ is the union of a set of clutter measurements and a set of target generated measurements; the sets are assumed independent. The clutter is modeled as a PPP with intensity $\kappa(\mathbf{z}) = \lambda c(\mathbf{z})$. An extended target with state $\mathbf{x}$ is detected with state dependent probability of detection $p_{\mathrm{D}}(\mathbf{x})$, and, if it is detected, the target measurements are modeled as a PPP with intensity $\gamma(\mathbf{x})\phi(\mathbf{z}|\mathbf{x})$, where both the Poisson rate $\gamma(\mathbf{x})$ and the spatial distribution $\phi(\mathbf{z}|\mathbf{x})$ are state dependent. A PPP with a probability of detection is sometimes called zero-inflated PPP.

For a nonempty set of measurements ($|\mathbf{Z}| > 0$), the conditional extended target measurement set likelihood is the product of the probability of detection and the PPP density

$$\ell_{\mathbf{Z}}(\mathbf{x}) = p_{\mathrm{D}}(\mathbf{x})p(\mathbf{Z}|\mathbf{x}) = p_{\mathrm{D}}(\mathbf{x})e^{-\gamma(\mathbf{x})}\prod_{\mathbf{z}\in\mathbf{Z}}\gamma(\mathbf{x})\phi(\mathbf{z}|\mathbf{x}). \tag{5}$$

The effective probability of detection for an extended target with state $\mathbf{x}$ is $p_{\mathrm{D}}(\mathbf{x})(1 - e^{-\gamma(\mathbf{x})})$, where $1 - e^{-\gamma(\mathbf{x})}$ is the Poisson probability of generating at least one detection. Accordingly, the effective probability of missed detection, i.e., the probability that the target is not detected, is

$$q_{\mathrm{D}}(\mathbf{x}) = 1 - p_{\mathrm{D}}(\mathbf{x}) + p_{\mathrm{D}}(\mathbf{x})e^{-\gamma(\mathbf{x})}. \tag{6}$$

Note that $q_{\mathrm{D}}(\mathbf{x})$ is the conditional likelihood for an empty set of measurements, i.e., $\ell_{\emptyset}(\mathbf{x}) = q_{\mathrm{D}}(\mathbf{x})$ [cf. (5)].

Because of the unknown measurement origin,[3] it is necessary to discuss data association. Let the measurements in the set $\mathbf{Z}$ be indexed by $m \in \mathbb{M}$

$$\mathbf{Z} = \{\mathbf{z}^m\}_{m\in\mathbb{M}} \tag{7}$$

and let $\mathcal{A}^j$ be the space of all data associations A for the jth predicted global hypothesis, i.e., the jth predicted MB. A data association $A \in \mathcal{A}^j$ is an assignment of each measurement in $\mathbf{Z}$ to a source, either to the *background* (clutter or new target) or to one of the existing targets indexed by $\mathbb{I}^j$. Note that $\mathbb{M} \cap \mathbb{I}^j = \emptyset$ for all j.

The space of all data associations for the jth hypothesis is $\mathcal{A}^j = \mathcal{P}(\mathbb{M} \cup \mathbb{I}^j)$, i.e., a data association $A \in \mathcal{A}^j$ is a partition of $\mathbb{M} \cup \mathbb{I}^j$ into nonempty disjoint subsets $C \in A$, called index cells.[4] Due to the standard MTT assumption that the targets generate measurements independent of each

[3] An inherent property of MTT is that it is unknown, which measurements are from targets and which are clutter, and among the target generated measurements it is unknown, which target generated which measurement. Hence, the update must handle this uncertainty.

[4] For example, let $\mathbb{M} = (m_1, m_2, m_3)$ and $\mathbb{I} = (i_1, i_2)$, i.e., three measurements and two targets. One valid partition of $\mathbb{M} \cap \mathbb{I}$, i.e., one of the possible associations, is $\{m_1, m_2, i_1\}, \{m_3\}, \{i_2\}$. The meaning of this is that measurements m_1, m_2 are associated to target i_1, target i_2 is not detected, and measurement m_3 is not associated to any previously detected target, i.e., measurement m_3 is either clutter or from a new target.

other, an index cell contains at most one target index, i.e., $|C \cap \mathbb{I}^j| \leq 1$ for all $C \in A$. Any association in which there is at least one cell, with at least two target indices, will have zero likelihood because this violates the independence assumption. If the index cell C contains a target index, then let i_C denote the corresponding target index. Furthermore, let $\mathbf{C}_C$ denote the measurement cell that corresponds to the index cell C, i.e., the set of measurements

$$\mathbf{C}_C = \bigcup_{m \in C \cap \mathbb{M}} \mathbf{z}^m. \tag{8}$$

C. Standard Dynamic Model

The existing targets—both the detected and the undetected—survive from time step k to time step $k+1$ with state dependent probability of survival $p_{\mathrm{S}}(\mathbf{x}_k)$. The target states evolve independently according to a Markov process with transition density $f_{k+1,k}(\mathbf{x}_{k+1}|\mathbf{x}_k)$. New targets appear independently of the targets that already exist. The target birth is assumed to be a PPP with intensity $D^b_{k+1}(\mathbf{x})$. In this paper, target spawning is omitted; for work on spawning in an extended target context see [18].

IV. PMBM FILTER

In this section, the PMBM conjugate prior for the standard extended object measurement and motion models are presented. Throughout the section time indexing is omitted for the sake of brevity.

A. PMBM Density

The PMBM model is a combination of a PPP and an MBM, where the PPP describes the distribution of the targets that are thus far undetected, and the MBM describes the distribution of the targets that have been detected at least once. Thus, the set of targets $\mathbf{X}$ can be divided into two disjoint subsets

$$\mathbf{X}^u,\ \mathbf{X}^d : \mathbf{X}^u \cup \mathbf{X}^d = \mathbf{X},\ \mathbf{X}^u \cap \mathbf{X}^d = \emptyset \tag{9}$$

corresponding to unknown targets $\mathbf{X}^u$, and detected targets $\mathbf{X}^d$. The PMBM set density can be expressed as

$$f(\mathbf{X}) = \sum_{\mathbf{X}^u \uplus \mathbf{X}^d = \mathbf{X}} f^u(\mathbf{X}^u) \sum_{j \in \mathbb{J}} \mathcal{W}^j f^j(\mathbf{X}^d) \tag{10a}$$

$$f^u(\mathbf{X}^u) = e^{-\langle D^u;1\rangle} \prod_{\mathbf{x} \in \mathbf{X}^u} D^u(\mathbf{x}) \tag{10b}$$

$$f^j(\mathbf{X}^d) = \sum_{\uplus_{i \in \mathbb{I}^j} \mathbf{X}^i = \mathbf{X}^d} \prod_{i \in \mathbb{I}^j} f^{j,i}\left(\mathbf{X}^i\right) \tag{10c}$$

where $f^{j,i}(\cdot)$ are Bernoulli set densities, defined in (3). There are $|\mathbb{J}|$ components in the MBM, the jth component has $|\mathbb{I}^j|$ Bernoulli components, and the probability of the jth MB component is $\mathcal{W}^j$. In target tracking each of the MB components in the mixture corresponds to a unique *global hypothesis* for the detected targets, i.e., a particular history of data associations for all detected targets.

The PMBM density is defined entirely by the parameters

$$D^u, \{(\mathcal{W}^j, \{(r^{j,i}, f^{j,i})\}_{i \in \mathbb{I}^j})\}_{j \in \mathbb{J}}. \tag{11}$$

Since the PMBM density is an MTT conjugate prior, performing prediction, and update means that we compute the new PMBM density parameters.

B. PMBM Filter Recursion

The PMBM filter consist of a prediction and an update step. The PMBM conjugate prediction is presented in Theorem 1.

THEOREM 1 Given a posterior PMBM density with parameters

$$D^u, \{(\mathcal{W}^j, \{(r^{j,i}, f^{j,i})\}_{i \in \mathbb{I}^j})\}_{j \in \mathbb{J}} \tag{12}$$

and the standard dynamic model (see Section III-C), the predicted density is a PMBM density with parameters

$$D^u_+, \{(\mathcal{W}^j_+, \{(r^{j,i}_+, f^{j,i}_+)\}_{i \in \mathbb{I}^j})\}_{j \in \mathbb{J}} \tag{13}$$

where

$$D^u_+(\mathbf{x}) = D^b(\mathbf{x}) + \left\langle D^u; p_{\mathrm{S}} f_{k+1,k} \right\rangle \tag{14a}$$

$$r^{j,i}_+ = \left\langle f^{j,i}; p_{\mathrm{S}} \right\rangle r^{j,i} \tag{14b}$$

$$f^{j,i}_+(\mathbf{x}) = \frac{\left\langle f^{j,i}; p_{\mathrm{S}} f_{k+1,k} \right\rangle}{\left\langle f^{j,i}; p_{\mathrm{S}} \right\rangle} \tag{14c}$$

and $\mathcal{W}^j_+ = \mathcal{W}^j$. ■

The proof of the theorem is omitted for brevity, details can be found in, e.g., [13]. The PMBM conjugate update is presented in Theorem 2.

THEOREM 2 Given a prior PMBM density with parameters

$$D^u_+, \{(\mathcal{W}^j_+, \{(r^{j,i}_+, f^{j,i}_+)\}_{i \in \mathbb{I}^j_+})\}_{j \in \mathbb{J}_+} \tag{15}$$

a set of measurements $\mathbf{Z}$, and the standard measurement model (see Section III-B), the updated density is a PMBM-density

$$f(\mathbf{X}|\mathbf{Z}) = \sum_{\mathbf{X}^u \uplus \mathbf{X}^d = \mathbf{X}} f^u(\mathbf{X}^u) \sum_{j \in \mathbb{J}_+} \sum_{A \in \mathcal{A}^j} \mathcal{W}^j_A f^j_A(\mathbf{X}^d) \tag{16a}$$

$$f^u(\mathbf{X}^u) = e^{-\langle D^u;1\rangle} \prod_{\mathbf{x} \in \mathbf{X}^u} D^u(\mathbf{x}) \tag{16b}$$

$$f^j_A(\mathbf{X}^d) = \sum_{\uplus_{C \in A} \mathbf{X}^C = \mathbf{X}} \prod_{C \in A} f^j_C(\mathbf{X}^C) \tag{16c}$$

where the weights are

$$\mathcal{W}^j_A = \frac{\mathcal{W}^j_+ \prod_{C \in A} \mathcal{L}_C}{\sum_{j' \in \mathbb{J}} \sum_{A' \in \mathcal{A}^{j'}} \mathcal{W}^{j'}_+ \prod_{C' \in A'} \mathcal{L}_{C'}} \tag{17a}$$

$$\mathcal{L}_C = \begin{cases} \kappa^{\mathbf{C}_C} + \left\langle D^u_+; \ell_{\mathbf{C}_C} \right\rangle & \text{if} C \cap \mathbb{I}^j = \emptyset, |\mathbf{C}_C| = 1 \\ \left\langle D^u_+; \ell_{\mathbf{C}_C} \right\rangle & \text{if} C \cap \mathbb{I}^j = \emptyset, |\mathbf{C}_C| > 1 \\ 1 - r^{j,i_C}_+ + r^{j,i_C}_+ \left\langle f^{j,i_C}_+; q_{\mathrm{D}} \right\rangle & \text{if } C \cap \mathbb{I}^j \neq \emptyset, \mathbf{C}_C = \emptyset \\ r^{j,i_C}_+ \left\langle f^{j,i_C}_+; \ell_{\mathbf{C}_C} \right\rangle & \text{if } C \cap \mathbb{I}^j \neq \emptyset, \mathbf{C}_C \neq \emptyset \end{cases} \tag{17b}$$

the densities $f_C^j(\mathbf{X})$ are Bernoulli densities with parameters

$$r_C^j = \begin{cases} \frac{\langle D_+^u;\ell_{\mathbf{C}_C}\rangle}{\kappa^{\mathbf{C}_C}+\langle D_+^u;\ell_{\mathbf{C}_C}\rangle} & \text{if} C\cap\mathbb{I}^j=\emptyset,\ |\mathbf{C}_C|=1 \\ 1 & \text{if} C\cap\mathbb{I}^j=\emptyset,\ |\mathbf{C}_C|>1 \\ \frac{r_+^{j,i_C}\left\langle f_+^{j,i_C};q_{\mathrm{D}}\right\rangle}{1-r_+^{j,i_C}+r_+^{j,i_C}\left\langle f_+^{j,i_C};q_{\mathrm{D}}\right\rangle} & \text{if} C\cap\mathbb{I}^j\neq\emptyset,\ \mathbf{C}_C=\emptyset \\ 1 & \text{if} C\cap\mathbb{I}^j\neq\emptyset,\ \mathbf{C}_C\neq\emptyset \end{cases} \tag{17c}$$

$$f_C^j(\mathbf{x}) = \begin{cases} \frac{\ell_{\mathbf{C}_C}(\mathbf{x})D_+^u(\mathbf{x})}{\langle D_+^u;\ell_{\mathbf{C}_C}\rangle} & \text{if} C\cap\mathbb{I}^j=\emptyset \\ \frac{q_{\mathrm{D}}(\mathbf{x})f_+^{j,i_C}(\mathbf{x})}{\left\langle f_+^{j,i_C};q_{\mathrm{D}}\right\rangle} & \text{if} C\cap\mathbb{I}^j\neq\emptyset,\ \mathbf{C}_C=\emptyset \\ \frac{\ell_{\mathbf{C}_C}(\mathbf{x})f_+^{j,i_C}(\mathbf{x})}{\left\langle f_+^{j,i_C};\ell_{\mathbf{C}_C}\right\rangle} & \text{if} C\cap\mathbb{I}^j\neq\emptyset,\ \mathbf{C}_C\neq\emptyset \end{cases} \tag{17d}$$

and the updated PPP intensity is $D^u(\mathbf{x}) = q_{\mathrm{D}}(\mathbf{x})D_+^u(\mathbf{x})$. ■

The proof of the theorem can be found in Appendix A. By comparing (16) with the PMBM density (10), we can immediately identify that we have a PMBM density. The number of components in the MBM increases, and contains one MB for every pair of predicted MB, $j\in\mathbb{J}_+$, and possible association, $A\in\mathcal{A}^j$.

V. COMPLEXITY, DATA ASSOCIATION APPROXIMATION, AND APPROXIMATION ERROR

Due to the unknown number of data associations, the number of components in the MBM grows rapidly as more data are observed, and it follows that the number of PMBM parameters increases. In this section, we first discuss the complexity of the PMBM filter. We then discuss methods that can be used to keep the number of MBM components at a tractable level, and finally, we discuss the approximation error that this reduction incurs.

A. Complexity

Each MB component in the MBM corresponds to a unique global hypothesis, where a global hypothesis was defined in Section IV-A as *a particular history of data associations for all detected targets*. The PMBM prediction preserves the number of MBs and the number of Bernoullis (see Theorem 1), however, due to the unknown data association, the update increases both these numbers.

In this section, we first give expressions for the number of possible data associations for a predicted MB, i.e., an expression for the cardinality of the set of data associations $\mathcal{A}^j$. Next, we present expressions for the number of MB components in the updated PMBM density, and for the number of unique Bernoulli components in the PMBM. Both the number of updated MBs and the number of unique updated Bernoullis contribute to the computational complexity: in theory, we should compute the probability of each of these MBs, and perform prediction and update operations for every unique Bernoulli. Finally, we discuss the complexity of the PMBM filter relative that of the δ-GLMB filter.

1) *Number of Data Associations:* Consider the jth predicted MB with Bernoullis indexed by $\mathbb{I}^j$, and a set of detections $\mathbf{Z}$. The number of possible ways in which the $|\mathbf{Z}|$ detections can be associated to either the $|\mathbb{I}^j|$ previously detected objects, or to the background (undetected object or false alarm), i.e., the size of the association space $\mathcal{A}^j$, is [19, Sec. 5]

$$N^{\mathcal{A}^j}(|\mathbf{Z}|,|\mathbb{I}^j|) = \sum_{C=1}^{|\mathbf{Z}|} \left\{ {|\mathbf{Z}| \atop C} \right\} \sum_{T=0}^{\min(C,|\mathbb{I}^j|)} \binom{C}{T} \frac{|\mathbb{I}^j|!}{(|\mathbb{I}^j|-T)!} \tag{18a}$$

where $\left\{ {\cdot \atop \cdot} \right\}$ and $\binom{\cdot}{\cdot}$ are defined in Table I. The complexity of the update is between exponential $\mathcal{O}(2^{|\mathbf{Z}|+|\mathbb{I}^j|})$ and factorial $\mathcal{O}((|\mathbf{Z}|+|\mathbb{I}^j|)!)$. For a predicted PMBM, indexed by $\mathbb{J}$, it follows that the total number of possible associations is

$$N^{\mathcal{A}} = \sum_{j\in\mathbb{J}} N^{\mathcal{A}^j}(|\mathbf{Z}|,|\mathbb{I}^j|). \tag{18b}$$

2) *Number of Components in MBM:* Using (18), we can recursively analyze how the number of global hypotheses changes with time. However, under certain conditions, it is possible to directly obtain an expression for the number of global hypotheses (MBs in the PMBM) at time k.

Let the probabilities of detection and survival be nonzero, $p_{\mathrm{D}}(\mathbf{x})\in(0,1]$ and $p_{\mathrm{S}}(\mathbf{x})\in(0,1]$, respectively. Let the birth intensity $D^b(\mathbf{x})>0$ and/or the initial undetected intensity $D^u(\mathbf{x})>0$. This corresponds to the following: targets can be detected; an existing target may remain in the surveillance area; new targets may be born; and there may be undetected targets in the surveillance area at initialization. In summary, this means that at any time step k, there may be targets in the surveillance area, that may cause detections. Finally, let the PMBM filter be initialized at time $k=0$ with $\mathbb{J}_0=\{j_1\}$, $\mathcal{W}_0^{j_1}=1$, and $\mathbb{I}_0^{j_1}=\emptyset$, i.e., an empty MBM. This corresponds to zero previously detected targets at initialization.

Given a measurement set $\mathbf{Z}_1$ at time $k=1$, the number of MB components in the updated PMBM density is given by the number of associations

$$|\mathbb{J}_{1|1}| = N^{\mathcal{A}^{j_1}}(|\mathbf{Z}_1|,0) = \sum_{C=1}^{|\mathbf{Z}_1|} \left\{ {|\mathbf{Z}_1| \atop C} \right\} = B(|\mathbf{Z}_1|) \tag{19}$$

where the last equality is a standard relation between the Stiriling numbers and the Bell numbers, see, e.g., [20]. In other words, the number of MBs is given by the Bell number of order $|\mathbf{Z}_1|$. It can be shown that the number of MBM components, given measurement sets up to and including time step k and an empty initial MBM, is given by the Bell number whose order n is the sum of the measurement set cardinalities

$$|\mathbb{J}_{k|k}| = |\mathbb{J}_{k+1|k}| = B\left(\sum_{t=1}^{k}|\mathbf{Z}_t|\right) = B\left(\left|\mathbf{Z}^k\right|\right). \tag{20}$$

Importantly, this is the same as the number of ways that we can partition $\mathbf{Z}^k=\cup_{t=1}^k\mathbf{Z}_t$ [21]. The sequence of Bell

numbers $B(n)$ is log-convex,[5] and $B(n)$ grows very rapidly. For example, for two measurements sets $\mathbf{Z}_1$ and $\mathbf{Z}_2$, both with two measurements, there are $B(2+2) = 15$ hypotheses. A small increase in the number of detections per time step to four (twice the amount), results in an MBM with $B(4+4) = 4140$ hypotheses.

Each MB corresponds to a unique global hypothesis. However, two (or more) MBs may contain identical Bernoulli components, i.e., the histories of data associations may be identical for a pair of Bernoullis in the two MBs. The number of unique Bernoullis at time step k is the number of possible subsets of $\mathbf{Z}^k$

$$N_k^B = 2^{|\mathbf{Z}^k|}. \tag{21}$$

This describes the number of Bernoulli predictions, cf. (14b) and (14c), and Bernoulli updates, cf. (17c) and (17d), that are required in the (exact) PMBM filter.

3) *Discussion:* Here, we discuss the complexity of the PMBM filter in relation to that of the δ-GLMB filter. First, note that the global hypotheses may contain Bernoulli components with uncertain existence, i.e., $r < 1$. From each global hypothesis with uncertain target existences, global hypotheses with certain target existence can easily be found. A single Bernoulli with probability of existence $r < 1$ and state density $f(\mathbf{x})$ can be expanded into a Bernoulli mixture density $f_{\text{ce}}(\cdot)$ that has two hypotheses

$$f_{\text{ce}}(\mathbf{X}) = (1-r) f_1(\mathbf{X}) + r f_2(\mathbf{X}) \tag{22}$$

where $f_1(\mathbf{X})$ and $f_2(\mathbf{X})$ are Bernoulli densities with probabilities of existence $r_1 = 0$ and $r_2 = 1$, respectively, and state densities $f_1(\mathbf{x}) = f_2(\mathbf{x}) = f(\mathbf{x})$. Generalizing this, an MB process with s components with uncertain existence (i.e., $r < 1$) can be represented by a mixture of 2^s MB processes with certain existences (i.e., each Bernoulli in the MB has either $r = 0$ or $r = 1$). In [14, Sec. 4.A], such an MBM density representation with certain target existence is denoted MBM_{01}.

A δ-GLMB density and a uniquely labelled MBM_{01} density can represent the same labelled multitarget densities with the same number of global hypotheses, in which target existence is certain [14, Prop. 7]. An MBM_{01} has a significantly higher number of hypotheses, compared to the corresponding MBM [14, Sec. 4]; having fewer global hypotheses is advantageous because it translates to a lower computational cost. In the update, the more global hypotheses there are, the more data association weights (17a) have to be computed. Regarding the prediction, the PMBM prediction can be implemented without approximation; the prediction of the δ-GLMB density, which has certain target existence, results in an increase of the number of global hypotheses and, thus, requires approximation using the k-shortest paths algorithm, see [9] and the discussion in [14, Sec. 4].

For point targets, simulation studies have shown that a better tradeoff between the tracking performance and the computational cost is obtained when global hypotheses with uncertain existence are used [15]. The same conclusion can be drawn for extended targets based on the results of the simulation study presented in Section VII.

B. Approximations of the Data Association Problem

To achieve computational tractability, it is necessary to reduce the number of PMBM parameters. Here, we will briefly describe the strategy for doing this that was used to obtain the results presented in Section VII. First, the number of data associations is reduced using gating, clustering, and ranking of the association events. Second, after an updated PMBM has been computed, we reduce the number of parameters using pruning, merging, and recycling.

1) *Reducing the Number of Associations:* First, gating, described in, e.g., [24, Sec. 2.2.2.2], is performed; naturally the extended target gates take into account both the position and the extent of the target, as well as state uncertainties. Given the gating, the targets and the measurements are separated into approximately independent subgroups, using a method similar to the one proposed in [25, Sec. 3]. After the grouping, we use the methods proposed in [7] and [8] to compute several different partitionings of the measurements. Finally, for each partitioning we compute the M best assignments using Murty's algorithm [26]. This three step procedure—gating, partitioning, assignment—results in a subset of associations $\hat{\mathcal{A}} \subseteq \mathcal{A}$, and typically reduces the number of associations in the update by several orders of magnitude. Similar approaches to reducing the number of data associations have been used previously in several extended target tracking filters, see [6]–[9]. As an alternative to using partitioning and assignment to find a subset of associations, random sampling methods can be used; this is explored in [19], [21], and [27].

2) *Reducing the Number of Parameters:* After the PMBM update, MBM components whose updated weight fall below a threshold are pruned from the MBM. For the remaining MBM components, we apply the recycling method suggested in [28] and [29]. All Bernoullis with probability of existence below a threshold τ_{rec} are removed from the MBM, approximated as a PPP with intensity $r f(\mathbf{x})$, and this intensity is added to the updated undetected PPP density. If the PPP intensity is represented by a distribution mixture, which is the typical case, then similar mixture components can be merged, e.g., by minimising the Kullback–Leibler divergence (KL-div), and mixture components with low weights can be pruned from the PPP intensity. Finally, we apply the merging algorithm outlined in Section V-C to the MBM.

C. MBM Merging

In [30], an approximate Poisson MB filter for point target tracking is proposed, where the PMBM density that

[5]The sequence of Bell numbers is logarithmically convex, i.e., $B(n)^2 \leq B(n-1)B(n+1)$ for $n \geq 1$ [22]. If the Bell numbers are divided by the factorials, $\frac{B(n)}{n!}$, the sequence is logarithmically concave, $(\frac{B(n)}{n!})^2 \geq \frac{B(n-1)}{(n-1)!}\frac{B(n+1)}{(n+1)!}$, for $n \geq 1$ [23].

results after the update is approximated as a PMB density by using variational approximation to minimize the KL-div between the true PMBM density and the approximate PMB density. Empirically, we have found that in extended object filtering it is generally not advisable to merge the whole PMBM density to a single PMB density. The main reason is the extent: merging two densities with significantly different extent estimates will result in an approximate density in which the extent estimates are distorted. However, in extended target tracking, similar components in the PMBM density can be merged, in order to reduce the computational cost of the PMBM filter.

Consider an MBM density with MB components indexed by the index set $\mathbb{J}$. The KL-div between two MB densities $j_1 \in \mathbb{J}$ and $j_2 \in \mathbb{J}$, with equal number of Bernoulli components $|\mathbb{I}^{j_1}| = |\mathbb{I}^{j_2}|$, is upper bounded [30]

$$D\left(f^{j_1}||f^{j_2}\right) \leq \sum_{\pi\in\Pi} q(\pi) \prod_{i\in\mathbb{I}^{j_1}} \int f^{j_1,i}(\mathbf{X}^i) \log\left(q(\pi)\frac{f^{j_1,i}(\mathbf{X}^i)}{f^{j_2,\pi(i)}(\mathbf{X}^i)}\right)\delta\mathbf{X}^i \tag{23}$$

where Π is the set of all ways to assign the Bernoulli components indexed by $\mathbb{I}^{j_1}$ to the Bernoulli components indexed by $\mathbb{I}^{j_2}$, and $q(\pi) \in [0, 1]$ are weights for the assignments π, $\sum_{\pi\in\Pi} q(\pi) = 1$; for additional details, see [30].

For two MB densities, we compute the pairwise kl-div between the Bernoulli densities, and compute an assignment $\hat{\pi}$ that gives the minimal sum of KL-div. Setting $q(\hat{\pi}) = 1$, we get

$$\begin{aligned} &D\left(f^{j_1}||f^{j_2}\right) && (24)\\ &\quad\leq \prod_{i\in\mathbb{I}^{j_1}} \int f^{j_1,i}(\mathbf{X}^i) \log\left(\frac{f^{j_1,i}(\mathbf{X}^i)}{f^{j_2,\hat{\pi}(i)}(\mathbf{X}^i)}\right)\delta\mathbf{X}^i \\ &\quad= D_{\mathrm{UB}}\left(f^{j_1}||f^{j_2}\right) && (25)\end{aligned}$$

where the subscript UB denotes the upper bound. In this paper, we use MBM merging and merge MB densities for which $D_{\mathrm{UB}}\left(f^{j_1}||f^{j_2}\right)$ is smaller than a threshold.

D. Approximation Error

The PMBM density (10) can be rewritten as a mixture of Poisson MB densities

$$f(\mathbf{X}) = \sum_{j\in\mathbb{J}} \mathcal{W}^j \sum_{\mathbf{X}^u \uplus \mathbf{X}^d = \mathbf{X}} f^u(\mathbf{X}^u) f^j(\mathbf{X}^d) \tag{26}$$

where the Poisson density $f^u(\mathbf{X}^u)$ is equal for all components. Using gating, partitioning, and assignment, we seek to prune low weight components from the mixture density, such that only components with significant weights remain. Trivially, pruning updated MBM components with low weights would achieve precisely this. Let

$$f_{\mathbb{J}}(\mathbf{X}) = \sum_{j\in\mathbb{J}} \mathcal{W}^j f^j(\mathbf{X}), \quad f_{\mathbb{H}}(\mathbf{X}) = \sum_{j\in\mathbb{H}} \mathcal{W}^j f^j(\mathbf{X}) \tag{27}$$

be two unnormalized PMBM densities with nonnegative weights (i.e., the weights do not necessarily sum to one). If $\mathbb{H} \subseteq \mathbb{J}$, then [31, Prop. 5] shows that the L_1-error incurred when approximating $f_{\mathbb{J}}(\mathbf{X})$ with $f_{\mathbb{H}}(\mathbf{X})$ satisfies

$$\|f_{\mathbb{J}} - f_{\mathbb{H}}\|_1 = \sum_{j\in\mathbb{J}\setminus\mathbb{H}} \mathcal{W}_j \tag{28a}$$

$$\left\| \frac{f_{\mathbb{J}}}{\|f_{\mathbb{J}}\|_1} - \frac{f_{\mathbb{H}}}{\|f_{\mathbb{H}}\|_1} \right\|_1 \leq 2\frac{\|f_{\mathbb{J}}\|_1 - \|f_{\mathbb{H}}\|_1}{\|f_{\mathbb{J}}\|_1}. \tag{28b}$$

This result supports the intuitive idea that keeping components with large weights, and discarding components with minimal weights, will yield a small L_1-error. Furthermore, this shows us that it is possible to achieve an arbitrarily accurate approximation by keeping more components, which in turn shows us that conjugate priors based on MB densities may be useful even though the theoretical growth of the number of components is hyperexponential. After pruning PMBM components, the approximate density is normalized. Assuming that $f_{\mathbb{J}}$ is normalized and its approximation $f_{\mathbb{H}}$ is not, (28b) shows that the L_1-error for the normalized approximation is less than two times the sum of the truncated weights. Further analysis of the approximation error is presented in [19].

In [13], it is shown that the minimum Kullback–Liebler divergence PPP approximation of a Bernoulli density is a PPP whose intensity is equal to the product of the Bernoulli existence probability and state density. In other words, the recycling in Section V-B2 minimizes the KL-div. Setting the recycling threshold $\tau_{\mathrm{rec}} = 0.1$ is suggested in [28] and [29], where it is shown to give small KL-div errors. Similarly, by choosing a low threshold in the MB merging algorithm, we guarantee that the resulting approximation error has low error. Finally, using a reasoning similar to (28), it can be shown that pruning the PPP intensity by removing low weight components, and merging similar components by minimizing the KL-div, incurs a small error.

VI. GGIW IMPLEMENTATION

In this section, an implementation of the PMBM filter is presented. There are several single extended target models available in the literature, see [1] for an overview. Here we have chosen the random matrix model [32], [33], in which the target shape is approximated by an ellipse. The random matrix model is relatively simple to use, yet flexible enough to be applicable to data from radar [34], [35], Lidar [8], [19], [27], [36], and camera [37]. With the random matrix model, it is possible to handle noisy nonlinear measurement models, e.g., noisy polar measurements [38]–[41]; in these cases the data are preprocessed with a polar-to-Cartesian transformation. Furthermore, the random matrix model has been used in many other multiple extended target tracking filters, making comparison easy. A comprehensive discussion of the random matrix model is given in [1, Sec. 3].

A. Single Target Models

In the random matrix model, the extended target state $\mathbf{x}_k$ is the combination of the scalar γ_k, the vector $\boldsymbol{\xi}_k$, and the matrix X_k. The random vector $\boldsymbol{\xi}_k \in \mathbb{R}^{n_x}$ is the kinematic state, which describes the target's position and its motion

TABLE II
GGIW Update

Input: GGIW parameter ζ_+, set of detections $\mathbf{W}$, measurement model H.
Output: Updated GGIW parameter ζ and predicted likelihood ℓ:

$$\zeta = \begin{cases} \alpha &= \alpha_+ + |\mathbf{W}|, \\ \beta &= \beta_+ + 1, \\ \mathbf{m} &= \mathbf{m}_+ + K\varepsilon, \\ P &= P_+ - KHP_+, \\ v &= v_+ + |\mathbf{W}|, \\ V &= V_+ + N + Z \end{cases}$$

where

$$\begin{aligned} \bar{\mathbf{z}} &= \tfrac{1}{|\mathbf{W}|}\textstyle\sum_{\mathbf{z}^i\in\mathbf{W}} \mathbf{z}^i, \\ Z &= \textstyle\sum_{\mathbf{z}^i\in\mathbf{W}} \left(\mathbf{z}^i - \bar{\mathbf{z}}\right)\left(\mathbf{z}^i - \bar{\mathbf{z}}\right)^{\mathrm{T}} \\ \hat{X} &= V_+ \left(v_+ - 2d - 2\right)^{-1}, \\ \varepsilon &= \bar{\mathbf{z}} - H\mathbf{m}_+, \\ S &= HP_+H^{\mathrm{T}} + \tfrac{\hat{X}}{|\mathbf{W}|}, \\ K &= P_+H^{\mathrm{T}}\left(S\right)^{-1}, \\ N &= \hat{X}^{1/2}S^{-1/2}\varepsilon\varepsilon^{\mathrm{T}}S^{-\mathrm{T}/2}\hat{X}^{\mathrm{T}/2} \end{aligned}$$

Predicted likelihood, where $\Gamma(\cdot)$ is the Gamma function, and $\Gamma_d(\cdot)$ is the multivariate Gamma function,

$$\ell = \left(\pi^{|\mathbf{W}|}|\mathbf{W}|\right)^{-\frac{d}{2}} \frac{|V_+|^{\frac{v_+-d-1}{2}}\Gamma_d\left(\frac{v-d-1}{2}\right)\left|\hat{X}\right|^{\frac{1}{2}}\Gamma\left(\alpha\right)\left(\beta_+\right)^{\alpha_+}}{|V|^{\frac{v-d-1}{2}}\Gamma_d\left(\frac{v_+-d-1}{2}\right)|S|^{\frac{1}{2}}\Gamma\left(\alpha_+\right)\left(\beta\right)^{\alpha}}$$

TABLE III
GGIW Prediction

Input: GGIW parameter ζ, motion model $g(\cdot)$, process noise covariance Q, transformation matrix $M(\cdot)$, sampling time T_s, maneuvering correlation constant τ, measurement rate parameter η.
Output: Predicted GGIW parameter ζ_+, where $G = \nabla_{\boldsymbol{\xi}} g(\boldsymbol{\xi})\big|_{\boldsymbol{\xi}=\mathbf{m}}$,

$$\zeta_+ = \begin{cases} \alpha_+ &= \frac{\alpha}{\eta}, \\ \beta_+ &= \frac{\beta}{\eta}, \\ \mathbf{m}_+ &= g\left(\mathbf{m}\right), \\ P_+ &= GPG^{\mathrm{T}} + Q, \\ v_+ &= 2d + 2 + e^{-T_s/\tau}\left(v - 2d - 2\right), \\ V_+ &= e^{-T_s/\tau}M\left(\mathbf{m}\right)VM\left(\mathbf{m}\right)^{\mathrm{T}} \end{cases}$$

TABLE IV
Assumptions

- GGIW birth PPP intensity with known parameters,

$$D^b_{k+1}(\mathbf{x}) = \textstyle\sum_{n=1}^{N^b_{k+1}} w^{b,n}_{k+1}\mathcal{GGIW}\left(\mathbf{x}_{k+1}\,;\,\zeta^{b,n}_{k+1}\right). \quad t \tag{33}$$

- GGIW initial undetected PPP intensity with known parameters,

$$D^u_0(\mathbf{x}) = \sum_{n=1}^{N^u_0} w^{u,n}_0\mathcal{GGIW}\left(\mathbf{x}_0\,;\,\zeta^{u,n}_0\right). \tag{34}$$

- Empty initial MBM: $\mathbb{J}_0 = \{j_1\}$, $\mathcal{W}^{j_1}_0 = 1$, and $\mathbb{I}^{j_1}_0 = \emptyset$.
- Probabilitites of detection and survival can be approximated as

$$p_{\mathrm{D}}(\mathbf{x})f(\mathbf{x}) \approx p_{\mathrm{D}}(\hat{\mathbf{x}})f(\mathbf{x}), \qquad p_{\mathrm{S}}(\mathbf{x})f(\mathbf{x}) \approx p_{\mathrm{S}}(\hat{\mathbf{x}})f(\mathbf{x}). \tag{35}$$

  where $\hat{\mathbf{x}} = \mathbb{E}[\mathbf{x}] = \int \mathbf{x}f(\mathbf{x})\mathrm{d}\mathbf{x}$.
- Clutter Poisson rate λ is known and the spatial distribution is uniform, $c(\mathbf{z}) = \mathrm{A}^{-1}$, where A is the volume of the surveillance region.

parameters (e.g., velocity, acceleration, and turn-rate). The random matrix $X_k \in \mathbb{S}^d_{++}$ is the extent state and describes the target's size and shape, and d is the dimension of the extent (typically $d = 2$ or $d = 3$). Finally, the random variable $\gamma_k > 0$ is the measurement model Poisson rate.

The measurement likelihood for a single measurement $\mathbf{z}$, cf. (5), is

$$\phi(\mathbf{z}_k|\mathbf{x}_k) = \mathcal{N}\left(\mathbf{z}_k\,;\,H_k\boldsymbol{\xi}_k,\,X_k\right) \tag{29}$$

where H_k is a known measurement model. The single-target conjugate prior for the PPP model (5) with single measurement likelihood (29) is a GGIW distribution [33], [42]

$$\begin{aligned} f_{k|k}\left(\mathbf{x}\right) &= \mathcal{G}\left(\gamma_k\,;\,\alpha_{k|k},\,\beta_{k|k}\right)\mathcal{N}\left(\boldsymbol{\xi}_k\,;\,\mathbf{m}_{k|k},\,P_{k|k}\right) \\ &\quad\times\mathcal{IW}_d\left(X_k\,;\,v_{k|k},\,V_{k|k}\right) \qquad (30) \\ &= \mathcal{GGIW}\left(\mathbf{x}_k\,;\,\zeta_{k|k}\right) \qquad (31) \end{aligned}$$

where $\zeta_{k|k} = \left\{\alpha_{k|k},\,\beta_{k|k},\,m_{k|k},\,P_{k|k},\,v_{k|k},\,V_{k|k}\right\}$ is the set of GGIW density parameters. The gamma distribution is the conjugate prior for the unknown Poisson rate, and the Gaussian-inverse Wishart distributions are the conjugate priors for Gaussian distributed detections with unknown mean and covariance.

For a GGIW distribution with prior parameters $\zeta_{k|k-1}$, that is updated with a set of detections $\mathbf{W}$ under the linear Gaussian model (29), the updated parameters $\zeta_{k|k}$, and the corresponding predicted likelihood, are given in Table II. For further discussions about the measurement update within the random matrix extended target model see, e.g., [32], [33], [43].

The motion models are

$$\boldsymbol{\xi}_{k+1} = g\left(\boldsymbol{\xi}_k\right) + \mathbf{w}_k \tag{32a}$$

$$X_{k+1} = M(\boldsymbol{\xi}_k)X_kM(\boldsymbol{\xi}_k)^{\mathrm{T}} \tag{32b}$$

$$\gamma_{k+1} = \gamma_k \tag{32c}$$

where $g(\cdot)$ is a kinematic motion model, $\mathbf{w}_k$ is Gaussian process noise with zero mean and covariance Q, and $M(\boldsymbol{\xi}_k)$ is a transformation matrix. For these motion models, the predicted parameters $\zeta_{k+1|k}$ for a GGIW distribution with posterior parameters $\zeta_{k|k}$ are given in Table III. For longer discussions about prediction within the random matrix extended target model, see, e.g., [32], [33], [44].

B. Pseudo Code for the Update and the Prediction

The GGIW-PMBM filter propagates in time the GGIW-PMBM density parameters, using a recursion that consists of an update and a prediction. The assumptions are listed in Table IV. The assumptions about the probabilities of detection and survival hold trivially if $p_{\mathrm{D}}(\cdot)$ and $p_{\mathrm{S}}(\cdot)$ are constants, and the assumptions are expected to hold when $p_{\mathrm{D}}(\cdot)$ and $p_{\mathrm{S}}(\cdot)$ are sufficiently smooth functions within the uncertainty area of the estimate. Note that the assumptions of GGIW mixture intensities for the birth PPP and the initial undetected PPP result in all single target densities in the PMBM filter being GGIW densities, due to the conjugacy property.

The predicted GGIW-PMBM parameters are presented in Table V. The updated density for the undetected PPP has $N^b_{k+1} + N^u_{k|k}$ GGIW components after the prediction, whereas the number of MBM parameters remains the same as before the prediction. The pseudo-code for the PMBM update, under assumed GGIW models, is given in Table VI. This builds upon the PPP intensity updates for missed detection and detection, see Tables VII and VIII,

TABLE V
GGIW PMBM Prediction

Input: $D^u, \{(\mathcal{W}^j, \{(r^{j,i}, f^{j,i})\}_{i\in\mathbb{I}^j})\}_{j\in\mathbb{J}}$.
Output: $D^u_+, \{(\mathcal{W}^j_+, \{(r^{j,i}_+, f^{j,i}_+)\}_{i\in\mathbb{I}^j})\}_{j\in\mathbb{J}}$

$$
\begin{aligned}
D^u_+(\mathbf{x}) =& \sum_{n=1}^{N^b} w^{b,n}\mathcal{GGIW}\left(\mathbf{x}\,;\,\zeta^{b,n}\right) \\
&+ \sum_{n=1}^{N^u} w^{u,n} p_{\mathrm{S}}\left(\hat{\mathbf{x}}^{u,n}\right)\mathcal{GGIW}\left(\mathbf{x}\,;\,\zeta^{u,n}_+\right) \\
r^{j,i}_+ =& p_{\mathrm{S}}\left(\hat{\mathbf{x}}^{j,i}\right) r^{j,i} \\
f^{j,i}_+(\mathbf{x}) =& \mathcal{GGIW}\left(\mathbf{x}\,;\,\zeta^{j,i}_+\right)
\end{aligned}
$$

and $\mathcal{W}^j_+ = \mathcal{W}^j$, where $\zeta^{u,n}_+$ and $\zeta^{j,i}_+$ are computed as in Table III.

TABLE VI
GGIW-PMBM Update

Input: Predicted parameters $D^u_+, \{(\mathcal{W}^j_+, \{(r^{j,i}_+, f^{j,i}_+)\}_{i\in\mathbb{I}^j_+})\}_{j\in\mathbb{J}_+}$, measurement set $\mathbf{Z}$
Output: Updated parameters $D^u, \{(\mathcal{W}^j, \{(r^{j,i}, f^{j,i})\}_{i\in\mathbb{I}^j})\}_{j\in\mathbb{J}}$.
Compute D^u as in Table VII
Initialise: $\mathbb{J}\leftarrow\emptyset$, $j\leftarrow 0$
for $j_+\in\mathbb{J}_+$ **do**
  Compute subset of associations $\hat{\mathcal{A}}^{j_+}$
  for $A\in\hat{\mathcal{A}}^{j_+}$ **do**
    Increment: $j\leftarrow j+1$, $\mathbb{J}\leftarrow\mathbb{J}\cup j$
    Initialise: $\mathbb{I}^j\leftarrow\emptyset$, $i\leftarrow 0$, $\mathbb{D}\leftarrow\emptyset$, $\mathcal{L}^{j_+}_A\leftarrow 1$
    for $C\in A$ **do**
      Increment: $i\leftarrow i+1$, $\mathbb{I}^j\leftarrow\mathbb{I}^j\cup i$
      if $C\cap\mathbb{I}^{j_+}=\emptyset$ **then**
        From r^{j_+,i_C}, f^{j_+,i_C}, compute $r, f, \mathcal{L}$ as in Table VIII
      else
        From r^{j_+,i_C}, f^{j_+,i_C}, compute $r, f, \mathcal{L}$ as in Table IX
        $\mathbb{D}\leftarrow\mathbb{D}\cup i_C$
      end if
      $r^{j,i}\leftarrow r$, $f^{j,i}\leftarrow f$, $\mathcal{L}^{j_+}_A\leftarrow\mathcal{L}^{j_+}_A\times\mathcal{L}$
    end for
    for $i_+\in(\mathbb{I}^{j_+}\backslash\mathbb{D})$ **do**
      Increment: $i\leftarrow i+1$, $\mathbb{I}^j\leftarrow\mathbb{I}^j\cup i$
      From r^{j_+,i_C}, f^{j_+,i_C}, compute $r, f, \mathcal{L}$ as in Table X
      $r^{j,i}\leftarrow r$, $f^{j,i}\leftarrow f$, $\mathcal{L}^{j_+}_A\leftarrow\mathcal{L}^{j_+}_A\times\mathcal{L}$
    end for
    $\mathcal{W}^j\leftarrow\mathcal{L}^{j_+}_A$
  end for
end for
$\mathcal{W}^j\leftarrow\frac{\mathcal{W}^j}{\sum_{j'\in\mathbb{J}}\mathcal{W}^{j'}}$

TABLE VII
GGIW PPP Update: Missed Detection

Input: Predicted PPP intensity $D^u_+(\mathbf{x})$, probability of missed detection $q_{\mathrm{D}}(\mathbf{x})$.
Output: Updated PPP intensity $D^u(\mathbf{x})$:

$$D^u(\mathbf{x}) = \textstyle\sum_{n=1}^{N^u}\left(w_1^{u,n}\mathcal{GGIW}\left(\mathbf{x}\,;\,\zeta_1^{u,n}\right) + w_2^{u,n}\mathcal{GGIW}\left(\mathbf{x}\,;\,\zeta_2^{u,n}\right)\right)$$

where

$$
\begin{aligned}
w_1^{u,n} &= \left(1-p_{\mathrm{D}}\left(\hat{\mathbf{x}}^{u,n}\right)\right)w^{u,n} \\
w_2^{u,n} &= p_{\mathrm{D}}\left(\hat{\mathbf{x}}^{u,n}\right)\left(\frac{\beta^{u,n}_+}{\beta^{u,n}_+ + 1}\right)^{\alpha^{u,n}_+} w^{u,n} \\
\zeta_1^{u,n} &= \zeta_+^{u,n} \\
\zeta_2^{u,n} &= \{\alpha^{u,n}_+, \beta^{u,n}_+ + 1, \mathbf{m}^{u,n}_+, P^{u,n}_+, v^{u,n}_+, V^{u,n}_+\}
\end{aligned}
$$

TABLE VIII
GGIW PPP Update: Detection

Input: Predicted PPP intensity $D^u_+(\mathbf{x})$, and measurements set $\mathbf{C}$.
Output: Bernoulli parameters $r^u_{\mathbf{C}}$, $f^u_{\mathbf{C}}(\mathbf{x})$ and likelihood $\mathcal{L}^u_{\mathbf{C}}$:

$$
\begin{aligned}
r^u_{\mathbf{C}} &= \begin{cases} 1 & \text{if} \quad |\mathbf{C}|>1 \\ \frac{\mathcal{L}_{\mathbf{C}}}{\kappa^{\mathbf{C}}+\mathcal{L}_{\mathbf{C}}} & \text{if} \quad |\mathbf{C}|=1 \end{cases} \\
f^u_{\mathbf{C}}(\mathbf{x}) &= \frac{\sum_{n=1}^{N^u} w^{u,n} p_{\mathrm{D}}\left(\hat{\mathbf{x}}^{u,n}\right)\ell^{u,n}_{\mathbf{C}}\mathcal{GGIW}\left(\mathbf{x}\,;\,\zeta^{u,n}_{\mathbf{C}}\right)}{\sum_{n=1}^{N^u} w^{u,n} p_{\mathrm{D}}\left(\hat{\mathbf{x}}^{u,n}\right)\ell^{u,n}_{\mathbf{C}}} \\
\mathcal{L}^u_{\mathbf{C}} &= \sum_{n=1}^{N^u} w^{u,n} p_{\mathrm{D}}\left(\hat{\mathbf{x}}^{u,n}\right)\ell^{u,n}_{\mathbf{C}}
\end{aligned}
$$

where $\zeta^{u,n}_{\mathbf{C}}$ and $\ell^{u,n}_{\mathbf{C}}$ are computed as in Table II.

TABLE IX
GGIW Bernoulli Update: Detection

Input: Predicted Bernoulli parameters $r^{j,i}_+$, $f^{j,i}_+(\mathbf{x})$, and measurement set $\mathbf{C}$.
Output: Updated Bernoulli parameters $r^{j,i}_{\mathbf{C}}$, $f^{j,i}_{\mathbf{C}}(\mathbf{x})$, and likelihood $\mathcal{L}^{j,i}_{\mathbf{C}}$:

$$
\begin{aligned}
r^{j,i}_{\mathbf{C}} &= 1 \\
f^{j,i}_{\mathbf{C}}(\mathbf{x}) &= \mathcal{GGIW}\left(\mathbf{x}\,;\,\zeta^{j,i}_{\mathbf{C}}\right) \\
\mathcal{L}^{j,i}_{\mathbf{C}} &= r^{j,i}_+ p_{\mathrm{D}}\left(\hat{\mathbf{x}}^{j,i}\right)\ell^{j,i}_{\mathbf{C}}
\end{aligned}
$$

where $\zeta^{j,i}_{\mathbf{C}}$ and $\ell^{j,i}_{\mathbf{C}}$ are computed as in Table II.

TABLE X
GGIW Bernoulli Update: Missed Detection

Input: Predicted Bernoulli parameters $r^{j,i}$, $f^{j,i}(\mathbf{x})$.
Output: Updated Bernoulli parameters $r^{j,i}_\emptyset$, $f^{j,i}_\emptyset(\mathbf{x})$, and likelihood $\mathcal{L}^{j,i}_\emptyset$:

$$
\begin{aligned}
r^{j,i}_\emptyset &= \frac{r^{j,i}q^{j,i}_{\mathrm{D}}}{1-r^{j,i}+r^{j,i}q^{j,i}_{\mathrm{D}}} \\
f^{j,i}_\emptyset(\mathbf{x}) &= w_1^{j,i}\mathcal{GGIW}\left(\mathbf{x}_k\,;\,\zeta_1^{j,i}\right) + w_2^{j,i}\mathcal{GGIW}\left(\mathbf{x}_k\,;\,\zeta_2^{j,i}\right) \\
\mathcal{L}^{j,i}_\emptyset &= 1-r^{j,i}+r^{j,i}q^{j,i}_{\mathrm{D}}
\end{aligned}
$$

where

$$
\begin{aligned}
q^{j,i}_{\mathrm{D}} &= 1-p_{\mathrm{D}}\left(\hat{\mathbf{x}}^{j,i}\right)+p_{\mathrm{D}}\left(\hat{\mathbf{x}}^{j,i}\right)\left(\frac{\beta^{j,i}}{\beta^{j,i}+1}\right)^{\alpha^{j,i}} \\
w_1^{j,i} &= \left(q^{j,i}_{\mathrm{D}}\right)^{-1}\left(1-p_{\mathrm{D}}\left(\hat{\mathbf{x}}^{j,i}\right)\right) \\
w_2^{j,i} &= \left(q^{j,i}_{\mathrm{D}}\right)^{-1}p_{\mathrm{D}}\left(\hat{\mathbf{x}}^{j,i}\right)\left(\frac{\beta^{j,i}}{\beta^{j,i}+1}\right)^{\alpha^{j,i}} \\
\zeta_1^{j,i} &= \zeta^{j,i} \\
\zeta_2^{j,i} &= \{\alpha^{j,i}, \beta^{j,i}+1, m^{j,i}, P^{j,i}, v^{j,i}, V^{j,i}\}
\end{aligned}
$$

respectively, and the Bernoulli updates for detection and missed detection, see Tables IX and X, respectively.

The density for a target detected for the first time, see Table VII, is multimodal, with one mode for each of the GGIW components in the predicted PPP intensity D^u. Mixture reduction can be used to reduce this to a unimodal GGIW density [42], [45]. This reduction typically has low error, because one of the modes in the predicted PPP intensity is typically much likelier than the other modes.

The density for a previously detected target that is now missed, see Table X, is multimodal with two modes. This is due to the fact that there are two ways for the target detection to result in an empty measurement set. The first corresponds to the detection process modeled by $p_{\mathrm{D}}(\cdot)$, which may result in a missed detection. The second corresponds to the Poisson number of detections governed by the parameter γ, i.e., the Poisson random number of detections is zero.

Note that the Gaussian and inverse Wishart parameters are identical in both cases, it is only the gamma parameters that differ. Using gamma mixture reduction [42], the bimodality of the γ_k estimate can be reduced to a single mode.

For a predicted global hypothesis and a data association, any cluster of measurements not associated to a predicted target will initiate a new Bernoulli in the updated global hypothesis. After the update, as mentioned in Section V-B2, we check each updated global hypothesis and any Bernoullis with probability of existence below a threshold τ_{rec} are pruned.

VII. RESULTS

In this section, the results from a Monte Carlo simulation study, and experiments with laser range data, are presented.[6] A comparison between the PHD, CPHD, LMB, and δ-GLMB filters is presented in [9]. It shows that the LMB filter and the δ-GLMB filter outperform the PHD filter and the CPHD filter. Therefore, in the simulation study presented here, we focus on comparing the PMBM filter to the δ-GLMB filter and the LMB filter. In [9], two variants of the LMB filter are presented, one with known MB birth and one with an adaptive birth process. We found that the LMB filter with adaptive birth process performed better in the simulated scenarios, and have, therefore, chosen to only present those results. In both the PMBM filter and the δ-GLMB filter, the birth processes were tuned to fit the simulated scenarios well. Specifically, the birth processes were represented by a single Gaussian located at the center of the surveillance space, with a covariance chosen such that most of the surveillance area is within three standard deviations. In scenarios where the birth process cannot be tuned to the problem, birth processes with uniform position density can be used in both filters; for details on how to achieve this, see [46]. For further details about the δ-GLMB filter and the LMB filter, refer to [9].

The kinematic state is $\boldsymbol{\xi}_k = [\mathbf{p}_k,\ \mathbf{v}_k]^{\mathrm{T}} \in \mathbb{R}^4$ and describes the target's position $\mathbf{p}_k \in \mathbb{R}^2$ and velocity $\mathbf{v}_k \in \mathbb{R}^2$. The random matrix $X_k \in \mathbb{S}^2_{++}$ is two-dimensional (2-D). The motion model $g(\cdot)$ and process noise covariance Q are

$$g(\boldsymbol{\xi}_k) = \begin{bmatrix} \mathbf{I}_2 & T_s\mathbf{I}_2 \\ \mathbf{0}_2 & \mathbf{I}_2 \end{bmatrix} \boldsymbol{\xi}_k,\ Q = \mathbf{G}\sigma_a^2\mathbf{I}_2\mathbf{G}^{\mathrm{T}},\ \mathbf{G} = \begin{bmatrix} \frac{T_s^2}{2}\mathbf{I}_2 \\ T_s\mathbf{I}_2 \end{bmatrix}$$

where T_s is the sampling time and σ_a is the acceleration standard deviation. Because the kinematic state motion model is constant velocity, the extent transformation function M is an identity matrix, $M(\boldsymbol{\xi}_k) = \mathbf{I}_2$.

For GGIW-PMBM, we use Estimator 1 from [14, Sec. 6.A]: an estimate of the set of targets is obtained by taking the mean vector of all Bernoulli estimates with existence probability larger than 0.5 from the MB component with largest MB weight. For GGIW-δ-GLMB and GGIW-LMB, target extraction is performed analogously, see [9, Sec. 4.A.3] or [12, Sec. 6.E] for details. Further discussions of multitarget estimators can be found in [3, Sec. 14.5] and [14, Sec. 6].

For the performance evaluation of extended object estimates with ellipsoidal extents, a comparison study has shown that among six compared performance measures, the Gaussian Wasserstein distance (GWD) metric is the best choice [47]. The GWD is defined as [48]

$$d_{\text{GW}}(\mathbf{x}, \hat{\mathbf{x}}) = \|H\boldsymbol{\xi} - H\hat{\boldsymbol{\xi}}\|^2 + \operatorname{Tr}\left(X + \hat{X} - 2\left(X^{\frac{1}{2}}\hat{X}X^{\frac{1}{2}}\right)^{\frac{1}{2}}\right) \quad (36)$$

where the measurement model H picks out the position from the state vector. The GWD single target metric is integrated into the generalized optimal subpattern assignment (GOSPA) multi object metric [49], defined as

$$d_p^{(c,2)}(\mathbf{X}, \hat{\mathbf{X}}) = \left[\min_{\theta\in\Theta^{(|\mathbf{X}|,|\hat{\mathbf{X}}|)}} \sum_{(i,j)\in\theta} d_{\text{GW}}^{(c)}(\mathbf{x}^i, \hat{\mathbf{x}}^j)^p + \frac{c^p}{2}\left(|\mathbf{X}| - |\theta| + |\hat{\mathbf{X}}| - |\theta|\right)\right]^{\frac{1}{p}} \quad (37)$$

where $d_{\text{GW}}^{(c)}(\mathbf{x}^i, \hat{\mathbf{x}}^j) = \min(c\ ;\ d_{\text{GW}}(\mathbf{x}^i, \hat{\mathbf{x}}^j))$, $\Theta^{(|\mathbf{X}|,|\hat{\mathbf{X}}|)}$ is the set of all possible 2-D assignment sets, c denotes the cutoff at base distance, and p determines the severity of penalizing the outliers in the localisation component. Here we use $c = 10$, $p = 1$.

The GOSPA metric was proposed in [49] as a generalization of the OSPA metric [50] that allows a decomposition of the error into three parts: 1) localisation error $\sum_{(i,j)\in\theta} d_{\text{GW}}(\mathbf{x}^i, \hat{\mathbf{x}}^j)^p$, 2) missed targets (MT) $\frac{c^p}{2}(|\mathbf{X}| - |\theta|)$, and 3) false targets (FT) $\frac{c^p}{2}(|\hat{\mathbf{X}}| - |\theta|)$. For the simulation study, we present results for the following:

1) GOSPA (37);
2) normalized localisation error (NLE): localization error, divided by the number of localized targets, i.e., average localization error;
3) number of MT;
4) number of FT;
5) number of cardinality errors (CE): sum of MT and FT;
6) Time: the total time to process one full sequence of measurement sets.

GOSPA is important as a single unified performance metric; the other quantities are presented because they represent properties that are important in MTT.

A. Simulation Study

Three scenarios were simulated; the first two have been used in previous work to evaluate extended target tracking, see [6]–[9], the third was constructed for this paper. For each scenario, 100 Monte Carlo runs were performed, and the presented results are averaged over the Monte Carlo runs.

In the first scenario, two targets are simulated for 100 time steps. The true trajectories are shown in Fig. 1, the true

[6] All compared filters were implemented in MATLAB, and the simulations and experiments were run on a laptop with a 3.1 GHz Intel Core i7 processor and 16 Gb memory.

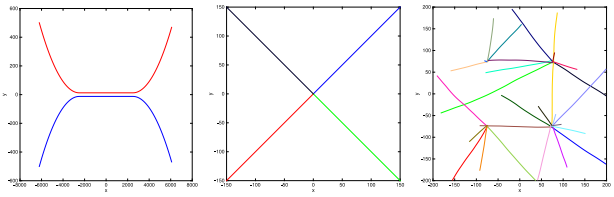

Fig. 1. True target tracks for the three simulated scenarios. In scenario 1 (left), the targets are born well separated, move close to each other, and then split. In scenario 2 (center), the targets are born from the same location, but at different times. In scenario 3 (right), there are four different birth locations.

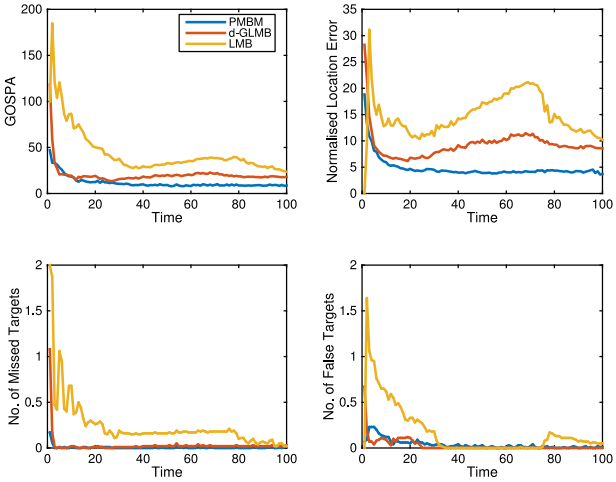

Fig. 2. Results for simulation scenario 1.

TABLE XI
Results for Simulation Scenario 1

Filter	PMBM	δ-GLMB	LMB
GOSPA	**1166**	2020	4411
NLE	**948**	1742	2350
MT	**0.63**	2.88	23.88
FT	3.73	**2.67**	17.34
CE	**4.36**	5.55	41.22
Time	46	177	**7**

The bold values indicate the best result in each row.

measurement rates were 10 and 20. The scenario parameters were set to $p_{\mathrm{D}} = 0.98$, $p_{\mathrm{S}} = 0.99$, and $\lambda = 30$. This scenario is challenging because when the targets are close their measurements form a single cluster, making the data association difficult. The GOSPA performance is shown in Fig. 2, and the numbers are summarized in Table XI. Overall, for this scenario the GOSPA results show that the PMBM filter gives smaller errors than both the δ-GLMB filter and the LMB filter. Noteworthy is that the localization error of the PMBM filter is unaffected when the targets are close and the data association is more complicated, whereas both the δ-GLMB filter and the LMB filter show increased localization errors when the targets are close.

In the second scenario, four targets were simulated for 200 time steps. The true trajectories are shown in Fig. 1, the true measurement rates were 4, 6, 8, and 10. The scenario parameters were set to $p_{\mathrm{D}} = 0.80$, $p_{\mathrm{S}} = 0.99$, and $\lambda = 30$. The targets appear at different times from the same birth

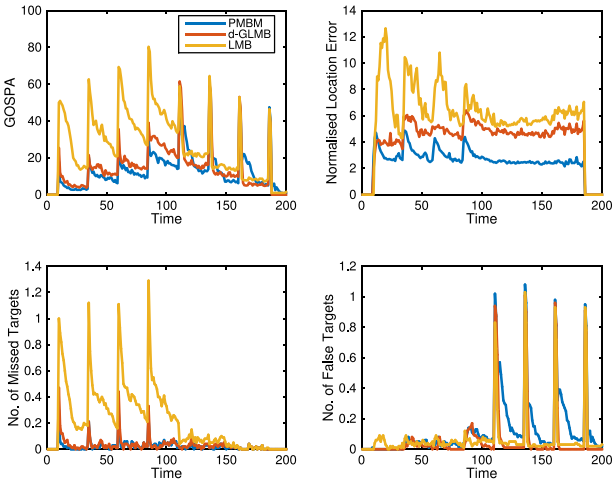

Fig. 3. Results for simulation scenario 2.

TABLE XII
Results for Simulation Scenario 2

Filter	PMBM	δ-GLMB	LMB
GOSPA	**2574**	2865	5274
NLE	**1149**	1963	2381
MT	**4.54**	6.16	44.15
FT	23.96	**11.88**	13.7
CE	28.5	**18.04**	57.85
Time	32	287	**8**

The bold values indicate the best result in each row.

location, and disappear at different times. This scenario illustrates how the different filters handle target birth and target death. The GOSPA performance is shown in Fig. 3, and the numbers are summarized in Table XII. The results show that for most time steps, the PMBM filter has lower GOSPA error. The PMBM filter has lower NLE and lower MT, however, it is also slower at removing targets that have disappeared, which can be seen in the FT results.

In the third scenario, 27 randomly generated targets were simulated for 100 time steps. The true trajectories are shown in Fig. 1, the true measurement rates were, for each target, randomly selected from $\{7, 8, 9\}$. The targets appear in, and disappear from, the surveillance area at different time steps. The parameters were set to $p_{\mathrm{D}} = 0.90$, $p_{\mathrm{S}} = 0.99$, and $\lambda = 60$. The birth spatial density consists of four GGIW components, with positions in $[\pm 75\ ,\ \pm 75]^{\mathrm{T}}$. This scenario illustrates how the different filters handle a higher target number and higher clutter density. The GOSPA performance is shown in Fig. 4, and the numbers are summarized in Table XIII.

In the third scenario, the LMB filter has larger GOSPA error, larger NLE, significantly larger MT, and lowest FT. Considering GOSPA error, Fig. 4 shows that δ-GLMB is slightly lower than PMBM until about time 70, when δ-GLMB starts to increase and becomes larger than PMBM. The NLE and MT are approximately the same for the PMBM filter and the δ-GLMB filter, except after time step 80 when there is a quite small difference in favour of the PMBM filter. For FT, the PMBM filter gives larger errors until about time step 70, when FT becomes larger for the

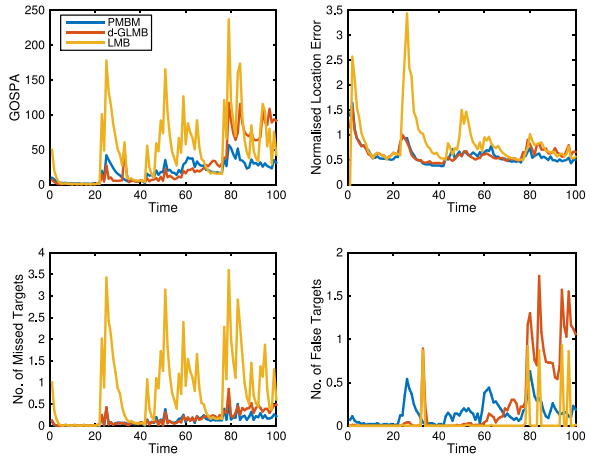

Fig. 4. Results for simulation scenario 3.

TABLE XIII
Results for Simulation Scenario 3

Filter	PMBM	δ-GLMB	LMB
GOSPA	**1892**	2753	4919
NLE	**556**	617	711
MT	**12.06**	16.18	79.62
FT	14.66	26.55	**4.54**
CE	**26.72**	42.73	84.16
Time	89	1450	**11**

The bold values indicate the best result in each row.

δ-GLMB filter. The PMBM filter's false targets are due to targets that disappear; the PMBM filter is slightly slower at removing disappeared targets, an effect that could also be observed in the second scenario. The increase in FT for the δ-GLMB filter starts around time step 60, when the number of targets in the scene increases to 10 or more. The rapid increase around time 80 corresponds to when the number of targets become larger than 15.

The computational cost of the PMBM filter is significantly lower than the cost of the δ-GLMB filter, but higher than the cost of the LMB filter. The LMB filter is faster than the PMBM filter because it maintains a single MB density, as opposed to the PMBM, which has a mixture of MB densities. However, the single MB density is also why the LMB filter has largest GWD-GOSPA error. That the PMBM is significantly faster than the δ-GLMB filter is mainly due to two reasons: 1) the PMBM has uncertain target existence, whereas the δ-GLMB has certain target existence, and 2) the PMBM is unlabelled that permits merging of similar MB densities.

To conclude, the simulation study shows that for the compared scenarios the PMBM filter achieves an appealing compromise between the computational cost and the tracking performance.

B. Experiment

An experiment with data from a 2-D Lidar sensor was performed. This dataset has previously been used for tracking using the GGIW-PHD filter [8]. The tracking results for detected targets are essentially identical for this data, since the measurements have relatively low measurement noise

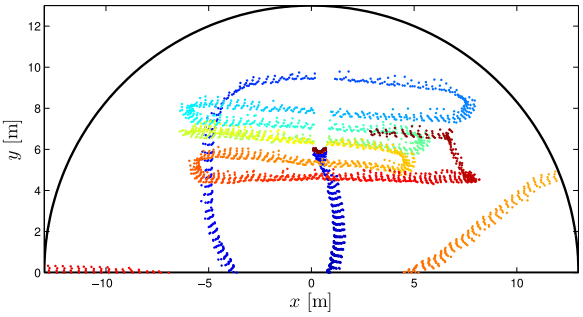

Fig. 5. 2-D laser range data, colors are used to visualise different time steps.

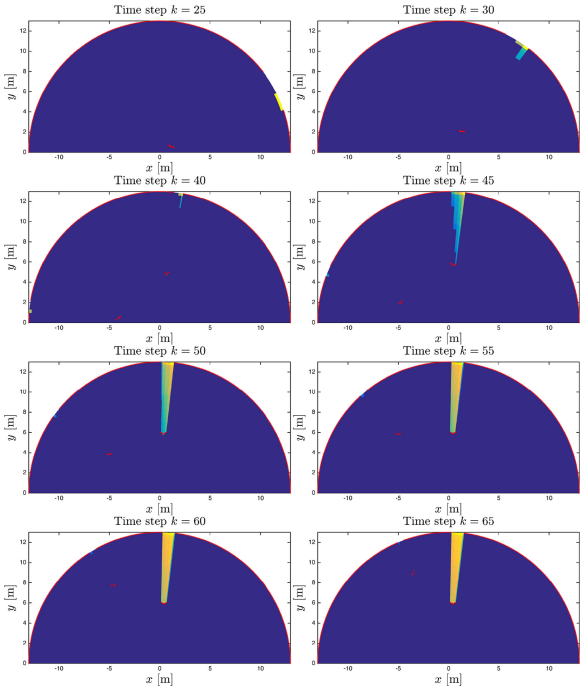

Fig. 6. PMBM tracking results, visualizing the position component of the PPP intensity for undetected targets. The red dots are the Lidar detections, blue color corresponds to low intensity, green corresponds to intermediate intensity, and yellow high intensity. When the pedestrian remains stationary, the PPP intensity increases behind them.

and there are very few clutter detections. Instead, the challenges posed by this data, and laser range data in general, are caused by occlusions since a Lidar cannot see behind a target. Because of this we emphasize here the estimation of the PPP density for undetected targets.

The data, shown in Fig. 5, contain four pedestrians, two of which remain in the surveillance area for a longer time. One pedestrian moves to the center of the surveillance area and remains there for the remainder of the experiment. The other pedestrian walks around in the surveillance area, both behind and in front of the first pedestrian. A pragmatic approach to handling the occlusions is to use a heterogeneous and time-variant probability of detection $p_{\mathrm{D}}(\mathbf{x})$. Such an approach was used in [8], and it makes it possible to keep track of targets while they are occluded. The method from [8] is used here, and the PPP intensity for undetected targets correctly captures the increased likelihood that a yet

undetected target is located in the occluded part of the surveillance area.

Results are shown in Fig. 6, where the position component of the undetected PPP intensity is shown. The area behind the stationary target is occluded for an extended period of time, and the PPP intensity correctly captures that in this area we can expect there to be undetected targets. The remaining parts of the surveillance volume, which is not occluded, has very low intensity, which is consistent with our expectation that there is not any undetected targets there.

VIII. CONCLUSION

This paper has presented a PMBM conjugate prior for tracking of multiple extended targets. Due to the unknown data associations, the complexity of the update is prohibitive, however, standard MTT methods such as gating and clustering can easily be used to handle this. A GGIW implementation is also presented, for tracking of extended targets with elliptic shapes. A simulation study shows that the PMBM filter compares well to the extended target δ-GLMB and LMB filters.

An experiment with laser range data illustrated how the Poisson process helps us to model undetected targets. That is, by approximating the probability of detection, the tracking filter can both track detected targets during occlusions, and represent parts of the surveillance area where yet undetected targets may be located. There are many more scenarios where the probability of detection varies in both time and space, creating a need to model undetected targets. Examples include sensors that scan the surveillance area in a nondeterministic way, such as radars with narrow lobes that can be focused on certain bearings, or optical sensors mounted on airborne vehicles.

Finally, note that labels can be used to form target trajectories from the output of the LMB and δ-GLMB filters. Using the PMBM filter output to form target trajectories is a topic for future work.

APPENDIX

In this appendix, we prove Theorem 2 using the probability generating functional (pgfl).

A. PGFL Background

In this section, we give a brief background on the pgfl. Let $\mathbf{X}$ be an RFS with multi-object density $f(\mathbf{X})$. The probability generating functional (pgfl) is a multitarget integral transform of the multiobject density. The PGFL and its inverse are defined as [3]

$$G[h] = \int h^{\mathbf{X}} f(\mathbf{X}) \delta\mathbf{X} \tag{38a}$$

$$f(\mathbf{X}) = \frac{\delta}{\delta \mathbf{X}} G[h]\Big|_{h=0} \tag{38b}$$

$$\frac{\delta}{\delta \mathbf{X}} G[h] = \frac{\delta^{|\mathbf{X}|}}{\prod_{\mathbf{x}\in\mathbf{X}} \delta\mathbf{x}} G[h] \tag{38c}$$

$$\frac{\delta}{\delta \mathbf{x}} G[h] \triangleq \lim_{\varepsilon \searrow 0} \frac{G[h + \varepsilon \delta_{\mathbf{x}}] - G[h]}{\varepsilon} \tag{38d}$$

where $h(\mathbf{x})$ is a test-function. The PPP, Bernoulli, and multi-Bernoulli pgfls, corresponding to the densities (2)–(4), respectively, are given by [3]

$$G^{\text{PPP}}[h] = \exp\left(\langle D; h\rangle - \langle D; 1\rangle\right) \tag{39}$$

$$G^{\text{Ber}}[h] = 1 - r + r\,\langle f; h\rangle \tag{40}$$

$$G^{\text{MB}}[h] = \prod_{i\in\mathbb{I}} \left(1 - r^i + r^i \left\langle f^i; h\right\rangle\right). \tag{41}$$

It follows from (38a) that the MBM pgfl is

$$G^{\text{MBM}}[h] = \sum_{j\in\mathbb{J}} \mathcal{W}^j \prod_{i\in\mathbb{I}^j} \left(1 - r^{j,i} + r^{j,i} \left\langle f^{j,i}; h\right\rangle\right). \tag{42}$$

Due to the standard independence assumption, see Section III-A2, the pgfl of the PMBM density (10) is given by

$$G[h] = G^u[h] \sum_{j\in\mathbb{J}} \mathcal{W}^j G^j[h] \tag{43a}$$

$$G^u[h] = \exp\left(\left\langle D^u; h\right\rangle - \left\langle D^u; 1\right\rangle\right) \tag{43b}$$

$$G^j[h] = \prod_{i\in\mathbb{I}^j} \left(1 - r^{j,i} + r^{j,i} \left\langle f^{j,i}; h\right\rangle\right). \tag{43c}$$

We rewrite this as

$$G[h] = \sum_{j\in\mathbb{J}} \mathcal{W}^j G^u[h] \prod_{i\in\mathbb{I}^j} G^{j,i}[h] \tag{44a}$$

$$G^{j,i}[h] = 1 - r^{j,i} + r^{j,i} \left\langle f^{j,i}; h\right\rangle. \tag{44b}$$

B. PGFL Form of Bayes Update

In this section, we present the Bayes update on pgfl form. Let $G_+[h]$ be the prior pgfl that corresponds to the multitarget density $f_+(\mathbf{X}) = f_{k|k-1}(\mathbf{X}_k|\mathbf{Z}^{k-1})$ in (1a). The pgfl for the measurement model (see Section III-B) with PPP clutter and PPP target measurements is

$$G[g|\mathbf{X}] = G^{\text{C}}[g] \left(1 - p_{\text{D}} + p_{\text{D}} \exp\left(\langle \gamma\phi; g - 1\rangle\right)\right)^{\mathbf{X}} \tag{45a}$$

$$G^{\text{C}}[g] = \exp\left(\langle \kappa; g - 1\rangle\right) \tag{45b}$$

where $g(\mathbf{z})$ is a test-function. The joint target and measurement pgfl is

$$F[g, h] = \int h^{\mathbf{X}} G[g|\mathbf{X}] f_+(\mathbf{X}) \delta\mathbf{X} \tag{46a}$$

$$= G^{\text{C}}[g] G_+[h\,(1 - p_{\text{D}} + p_{\text{D}} \exp\left(\gamma\,\langle\phi; g\rangle - \gamma\right))]. \tag{46b}$$

Assuming that the prior pgfl $G_+[h]$ is PMBM (43), and inserting into the joint pgfl (46) gives

$$F[g, h] = \sum_{j\in\mathbb{J}} \mathcal{W}^j F^j[g, h] \tag{47a}$$

$$F^j[g, h] = F^{\text{C}u}[g, h] \prod_{i\in\mathbb{I}^j} F^{j,i}[g, h] \tag{47b}$$

$$F^{\text{C}u}[g, h] = G^{\text{C}}[g] G^u_+[h(1 - p_{\text{D}} + p_{\text{D}} e^{\gamma\langle\phi;g\rangle - \gamma})] \tag{47c}$$

$$F^{j,i}[g, h] = G^{j,i}_+[h(1 - p_{\text{D}} + p_{\text{D}} e^{\gamma\langle\phi;g\rangle - \gamma})]. \tag{47d}$$

The updated pgfl $G[h]$ that corresponds to the Bayes updated density $f_{k|k}(\mathbf{X}_k|\mathbf{Z}^k)$ in (1b) is given by [3, pp. 530–531, Sec. 14.8.2]

$$G[h] = \frac{\frac{\delta F[g,h]}{\delta \mathbf{Z}}\Big|_{g=0}}{\frac{\delta F[g',h']}{\delta \mathbf{Z}}\Big|_{g'=0,h'=1}}. \tag{48}$$

C. Preliminaries to Proof of Theorem 2

In this section, we establish some preliminary results that will allow us to obtain the differentiation $\frac{\delta F[g,h]}{\delta \mathbf{Z}}$ that is needed in (48). From the sum rule for functional derivatives [3, p. 395], it holds that $\frac{\delta F[g,h]}{\delta \mathbf{Z}} = \sum_{j\in\mathbb{J}} \mathcal{W}^j \frac{\delta F^j[g,h]}{\delta \mathbf{Z}}$. From the product rule for functional derivatives [3, p. 395], it follows that the differentiation $\frac{\delta F^j[g,h]}{\delta \mathbf{Z}}$ consists of combinations of differentiations of $F^{\mathrm{C}u}[g,h]$ and of $F^{j,i}[g,h]$.

LEMMA 1

$$\frac{\delta \langle s; \exp(\gamma\ \langle \phi; g\rangle)\rangle}{\delta \mathbf{z}} = \langle s; \gamma \phi_{\mathbf{z}} \exp(\gamma\ \langle \phi; g\rangle)\rangle \tag{49}$$

where $s(\mathbf{x})$ is any function of $\mathbf{x}$ and $\phi_{\mathbf{z}} = \phi(\mathbf{z}|\mathbf{x})$.

Successive application of the chain rule for functional derivatives [3, p. 395] gives that

$$\frac{\delta \langle s; \exp(\gamma\ \langle \phi; g\rangle)\rangle}{\delta \mathbf{z}} = \left\langle s; \frac{\delta \exp(\gamma\ \langle \phi; g\rangle)}{\delta \mathbf{z}} \right\rangle \tag{50a}$$

$$= \langle s; \gamma \phi_{\mathbf{z}} \exp(\gamma\ \langle \phi; g\rangle)\rangle\,. \tag{50b}$$

This concludes the proof of Lemma 1.

LEMMA 2 The differentiation of $F^{\mathrm{C}u}[g,h]$ w.r.t. a single measurement $\mathbf{z}$ is

$$\frac{\delta F^{\mathrm{C}u}[g,h]}{\delta \mathbf{z}} = \left(\kappa(\mathbf{z}) + \left\langle h; D_+^u \ell_{\mathbf{z}} e^{\gamma\langle \phi; g\rangle}\right\rangle\right) F^{\mathrm{C}u}[g,h] \tag{51}$$

and the differentiation of $\kappa(\mathbf{z}) + \left\langle h; D_+^u \ell_{\mathbf{z}} e^{\gamma\langle \phi; g\rangle}\right\rangle$ w.r.t. a set of measurements $\mathbf{Y}$ is

$$\frac{\delta \left(\kappa(\mathbf{z}) + \left\langle h; D_+^u \ell_{\mathbf{z}} e^{\gamma\langle \phi; g\rangle}\right\rangle\right)}{\delta \mathbf{Y}} = \left\langle h; D_+^u \ell_{\mathbf{z}\cup\mathbf{Y}} e^{\gamma\langle \phi; g\rangle}\right\rangle. \tag{52}$$

The proof of (51) is given in [5, eq. (31) and (32)]. For the proof of (52), it follows from the sum rule for functional derivatives [3, p. 395] that

$$\frac{\delta \left(\kappa(\mathbf{z}) + \left\langle h; D_+^u \ell_{\mathbf{z}} e^{\gamma\langle \phi; g\rangle}\right\rangle\right)}{\delta \mathbf{Y}} = \frac{\delta \left\langle h; D_+^u \ell_{\mathbf{z}} e^{\gamma\langle \phi; g\rangle}\right\rangle}{\delta \mathbf{Y}} \tag{53}$$

and the equivalence of the RHS of (53) and the RHS of (52) follows from Lemma 1 and the definition of set derivative (38c). This concludes the proof of Lemma 2.

LEMMA 3 The differentiation of $F^{j,i}[g,h]$ w.r.t. a measurement set $\mathbf{Z}$ is

$$\frac{\delta F^{j,i}[g,h]}{\delta \mathbf{Z}} = r_+^{j,i} \left\langle h; f_+^{j,i} \ell_{\mathbf{Z}} e^{\gamma\langle \phi; g\rangle}\right\rangle. \tag{54}$$

It follows from the definition of $\langle\cdot;\cdot\rangle$, see Table I, and the sum rule for functional derivatives [3, p. 395] that

$$\frac{\delta F^{j,i}[g,h]}{\delta \mathbf{Z}} = r_+^{j,i} \frac{\delta \left(\left\langle f_+^{j,i} h p_{\mathrm{D}} e^{-\gamma}; e^{\gamma\langle \phi; g\rangle}\right\rangle\right)}{\delta \mathbf{Z}}. \tag{55}$$

This concludes the proof of Lemma 3.

LEMMA 4 The differentiation of $F^j[g,h]$ w.r.t. $\mathbf{Z}$ is

$$\frac{\delta F^j[g,h]}{\delta \mathbf{Z}} = F^{\mathrm{C}u}[g,h] \sum_{A\in\mathcal{A}^j} \prod_{C\in A} F_C^{'}[g,h] \tag{56a}$$

where

$$F_C^{'}[g,h] = \begin{cases} \kappa^{\mathbf{C}_C} + \left\langle h; D_+^u \ell_{\mathbf{C}_C} e^{\gamma\langle \phi; g\rangle}\right\rangle & \text{if} \quad C \cap \mathbb{I}_+^j = \emptyset, |\mathbf{C}_C| = 1 \\ \left\langle h; D_+^u \ell_{\mathbf{C}_C} e^{\gamma\langle \phi; g\rangle}\right\rangle & \text{if} \quad C \cap \mathbb{I}_+^j = \emptyset, |\mathbf{C}_C| > 1 \\ F^{j,i_C}[g,h] & \text{if} \quad C \cap \mathbb{I}_+^j \neq \emptyset, \mathbf{C}_C = \emptyset \\ r_+^{j,i_C} \left\langle h; f_+^{j,i_C} \ell_{\mathbf{C}_C} e^{\gamma\langle \phi; g\rangle}\right\rangle & \text{if} \quad C \cap \mathbb{I}_+^j \neq \emptyset, \mathbf{C}_C \neq \emptyset. \end{cases} \tag{56b}$$

The proof is by induction: For the initial step, assume that $\mathbb{M} = \{m_1\}$. Differentiation, Lemma 2 and Lemma 3, give

$$\frac{\delta F^j[g,h]}{\delta \mathbf{z}^{m_1}} = F^{\mathrm{C}u}[g,h] \left[\left(\kappa(\mathbf{z}) + \left\langle h; D_+^u \ell_{\mathbf{z}} e^{\gamma\langle \phi; g\rangle}\right\rangle\right) \prod_{i\in\mathbb{I}_+^j} F^{j,i}[g,h] + \sum_{\hat{\imath}\in\mathbb{I}_+^j} r_+^{j,\hat{\imath}} \left\langle h; f_+^{j,\hat{\imath}} \ell_{\mathbf{Z}} e^{\gamma\langle \phi; g\rangle}\right\rangle \prod_{i\in\mathbb{I}_+^j, i\neq\hat{\imath}} F^{j,i}[g,h] \right]. \tag{57}$$

We see that (57) is consistent with (56): we have the partitions of $\{m_1\} \cup \mathbb{I}_+^j$, for which there is at most one $i \in \mathbb{I}_+^j$ in each cell. The first row corresponds to a partition in which m_1 is placed in a cell of its own, $\{m_1\}, \{i_1\}, \ldots, \{i_I\}$, i.e., an association in which none of the previously detected targets are detected, and the single measurement is either from clutter or a new target. The second row corresponds to partitions $\{i_1\}, \ldots, \{m_1, \hat{\imath}\}, \ldots, \{i_I\}$, i.e., associations where the single measurement is associated to one of the existing targets.

Now, assume that we have established (56) for

$$\mathbb{M}_- = \{m_1, \ldots, m_{M-1}\} \tag{58}$$

and that we are to establish (56) for

$$\mathbb{M} = \{m_1, \ldots, m_{M-1}, m_M\}. \tag{59}$$

For the sake of notational clarity, let $\mathcal{A}_-^j$ be the association space corresponding to the index set $\mathbb{M}_-$, and let $\mathcal{A}^j$ be the association space corresponding to the index set $\mathbb{M}$.

Differentiation gives

$$\frac{\delta F^{\mathrm{C},u}[g,h]\sum_{A\in\mathcal{A}_-^j}\prod_{C\in A}F_C^{'}[g,h]}{\delta\mathbf{z}^{m_M}} = F^{\mathrm{C}u}[g,h]\left[\sum_{A\in\mathcal{A}_-^j}\sum_{\hat{C}\in A}\frac{\delta F_{\hat{C}}^{'}[g,h]}{\delta\mathbf{z}^{m_M}}\prod_{C\in A,C\neq\hat{C}}F_C^{'}[g,h] + \left(\kappa(\mathbf{z}^{m_M})+\left\langle h;D_+^u\ell_{\mathbf{z}^{m_M}}e^{\gamma\langle\phi;g\rangle}\right\rangle\right)\sum_{A\in\mathcal{A}_-^j}\prod_{C\in A}F_C^{'}[g,h]\right]. \tag{60}$$

The first row corresponds to new association partitions formed by adding the measurement index m_M to one of the existing cells in an association $A\in\mathcal{A}_-^j$, and the second row corresponds to new association partitions formed by putting m_M into a new cell and adding this cell to $A\in\mathcal{A}_-^j$. Together, this constitutes a summation over all possible ways to partition $\mathbb{M}\cup\mathbb{I}_+^j$, i.e., a summation over all associations in the association space $\mathcal{A}^j$, and (60) is, thus, consistent with (56). This concludes the proof of Lemma 4.

LEMMA 5 For scalar a, scalar b, function c and test function h, the following relation holds

$$a+b\langle h;c\rangle=\mathcal{L}(1-r+r\langle h;f\rangle) \tag{61a}$$

where

$$\mathcal{L}=a+b\langle c;1\rangle,\ r=\frac{b\langle c;1\rangle}{a+b\langle c;1\rangle},\ f=\frac{c}{\langle c;1\rangle}. \tag{61b}$$

The proof is trivial.

D. Proof of Theorem 2

In this section, we show that *a prior* PMBM pgfl $G_+[h]$ of the form (43) and the measurement model (45a) result in a PMBM pgfl that corresponds to the PMBM density given in Theorem 2. Let the set of measurements $\mathbf{Z}$ be indexed by the index set $\mathbb{M}$, $\mathbf{Z}=\{\mathbf{z}^m\}_{m\in\mathbb{M}}$. Differentiating, using Lemma 4, and setting $g=0$, we get

$$\left.\frac{\delta F[g,h]}{\delta\mathbf{Z}}\right|_{g=0}=F^{\mathrm{C},u}[0,h]\sum_{j\in\mathbb{J}}\mathcal{W}^j\sum_{A\in\mathcal{A}^j}\prod_{C\in A}F_C^{'}[0,h]. \tag{62}$$

where

$$F_C^{'}[0,h]=\begin{cases}\kappa^{\mathbf{C}_C}+\langle h;D_+^u\ell_{\mathbf{C}_C}\rangle & \text{if } C\cap\mathbb{I}_+^j=\emptyset,\ |\mathbf{C}_C|=1\\ \langle h;D_+^u\ell_{\mathbf{C}_C}\rangle & \text{if } C\cap\mathbb{I}_+^j=\emptyset,\ |\mathbf{C}_C|>1\\ 1-r_+^{j,i_C}+r_+^{j,i_C}\left\langle h;f_+^{j,i_C}q_{\mathrm{D}}\right\rangle & \text{if } C\cap\mathbb{I}_+^j\neq\emptyset,\ \mathbf{C}_C=\emptyset\\ r_+^{j,i_C}\left\langle h;f_+^{j,i_C}\ell_{\mathbf{C}_C}\right\rangle & \text{if } C\cap\mathbb{I}_+^j\neq\emptyset,\ \mathbf{C}_C\neq\emptyset.\end{cases} \tag{63}$$

Applying Lemma 5, we get

$$\left.\frac{\delta F[g,h]}{\delta\mathbf{Z}}\right|_{g=0}=F^{\mathrm{C},u}[0,h]\sum_{j\in\mathbb{J}}\sum_{A\in\mathcal{A}^j}\mathcal{W}^j\prod_{C\in A}\mathcal{L}_C(1-r_C+r_C\langle h;f_C\rangle) \tag{64}$$

where

$$\mathcal{L}_C=\begin{cases}\kappa^{\mathbf{C}_C}+\langle D_+^u;\ell_{\mathbf{C}_C}\rangle & \text{if } C\cap\mathbb{I}_+^j=\emptyset,\ |\mathbf{C}_C|=1\\ \langle D_+^u;\ell_{\mathbf{C}_C}\rangle & \text{if } C\cap\mathbb{I}_+^j=\emptyset,\ |\mathbf{C}_C|>1\\ 1-r_+^{j,i_C}+r_+^{j,i_C}\left\langle f_+^{j,i_C};q_{\mathrm{D}}\right\rangle & \text{if } C\cap\mathbb{I}_+^j\neq\emptyset,\ \mathbf{C}_C=\emptyset\\ r_+^{j,i_C}\left\langle f_+^{j,i_C};\ell_{\mathbf{C}_C}\right\rangle & \text{if } C\cap\mathbb{I}_+^j\neq\emptyset,\ \mathbf{C}_C\neq\emptyset\end{cases} \tag{65a}$$

$$r_C=\begin{cases}\frac{\langle D_+^u;\ell_{\mathbf{C}_C}\rangle}{\kappa^{\mathbf{C}_C}+\langle D_+^u;\ell_{\mathbf{C}_C}\rangle} & \text{if } C\cap\mathbb{I}_+^j=\emptyset,\ |\mathbf{C}_C|=1\\ 1 & \text{if } C\cap\mathbb{I}_+^j=\emptyset,\ |\mathbf{C}_C|>1\\ \frac{r_+^{j,i_C}\left\langle f_+^{j,i_C};q_{\mathrm{D}}\right\rangle}{1-r_+^{j,i_C}+r_+^{j,i_C}\left\langle f_+^{j,i_C};q_{\mathrm{D}}\right\rangle} & \text{if } C\cap\mathbb{I}_+^j\neq\emptyset,\ \mathbf{C}_C=\emptyset\\ 1 & \text{if } C\cap\mathbb{I}_+^j\neq\emptyset,\ \mathbf{C}_C\neq\emptyset\end{cases} \tag{65b}$$

$$f_C(\mathbf{x})=\begin{cases}\frac{D_+^u(\mathbf{x})\ell_{\mathbf{C}_C}(\mathbf{x})}{\langle D_+^u;\ell_{\mathbf{C}_C}\rangle} & \text{if } C\cap\mathbb{I}_+^j=\emptyset\\ \frac{f_+^{j,i_C}(\mathbf{x})q_{\mathrm{D}}(\mathbf{x})}{\left\langle f_+^{j,i_C};q_{\mathrm{D}}\right\rangle} & \text{if } C\cap\mathbb{I}_+^j\neq\emptyset,\ \mathbf{C}_C=\emptyset\\ \frac{f_+^{j,i_C}(\mathbf{x})\ell_{\mathbf{C}_C}(\mathbf{x})}{\left\langle f_+^{j,i_C};\ell_{\mathbf{C}_C}\right\rangle} & \text{if } C\cap\mathbb{I}_+^j\neq\emptyset,\ \mathbf{C}_C\neq\emptyset.\end{cases} \tag{65c}$$

Setting $h=1$ we get

$$\left.\frac{\delta F[g,h]}{\delta\mathbf{Z}}\right|_{g=0,h=1}=F^{\mathrm{C},u}[0,1]\sum_{j\in\mathbb{J}}\sum_{A\in\mathcal{A}^j}\mathcal{W}^j\prod_{C\in A}\mathcal{L}_C \tag{66}$$

and taking the ratio of (64) and (66), cf. (48), we get the pgfl of the Bayes updated density

$$G[h]=\frac{F^{\mathrm{C},u}[0,h]}{F^{\mathrm{C},u}[0,1]}\times\frac{\sum_{j\in\mathbb{J}}\sum_{A\in\mathcal{A}^j}\mathcal{W}^j\prod_{C\in A}\mathcal{L}_C(1-r_C+r_C\langle h;f_C\rangle)}{\sum_{j\in\mathbb{J}}\sum_{A\in\mathcal{A}^j}\mathcal{W}^j\prod_{C\in A}\mathcal{L}_C} \tag{67}$$

where the ratio

$$\frac{F^{\mathrm{C}u}[0,h]}{F^{\mathrm{C}u}[0,1]}=\exp\left\{\left\langle D^u;h\right\rangle-\left\langle D^u;1\right\rangle\right\} \tag{68a}$$

$$D^u(\mathbf{x})=q_{\mathrm{D}}(\mathbf{x})D_+^u(\mathbf{x}). \tag{68b}$$

We see that $G[h]$ in (67) is a product of (68a), which is the pgfl of a PPP with intensity (68b), and the pgfl of an MBM with parameters (65). This is consistent with Theorem 2, and concludes the proof.

REFERENCES

[1] K. Granström, M. Baum, and S. Reuter
Extended object tracking: Introduction, overview and applications
J. Adv. Inf. Fusion, vol. 12, no. 2, pp. 139–174, Dec. 2017.

[2] K. Gilholm, S. Godsill, S. Maskell, and D. Salmond
Poisson models for extended target and group tracking
Proc. SPIE, vol. 5913, pp. 230–241, Aug. 2005.

[3] R. Mahler
Statistical Multisource-Multitarget Information Fusion. Norwood, MA, USA: Artech House, 2007.

[4] R. Mahler
Advances in Multisource-Multitarget Information Fusion. Norwood, MA, USA: Artech House, 2014.

[5] R. Mahler
PHD filters for nonstandard targets, I: Extended targets
In *Proc. Int. Conf. Inf. Fusion*, Seattle, WA, USA, Jul. 2009, pp. 915–921.

[6] C. Lundquist, K. Granström, and U. Orguner
An extended target CPHD filter and a gamma Gaussian inverse Wishart implementation
IEEE J. Sel. Topics Signal Process., Special Issue Multi Target Tracking, vol. 7, no. 3, pp. 472–483, Jun. 2013.

[7] K. Granström, C. Lundquist, and U. Orguner
Extended target tracking using a Gaussian mixture PHD filter
IEEE Trans. Aerosp. Electron. Syst., vol. 48, no. 4, pp. 3268–3286, Oct. 2012.

[8] K. Granström and U. Orguner
A PHD filter for tracking multiple extended targets using random matrices
IEEE Trans. Signal Process., vol. 60, no. 11, pp. 5657–5671, Nov. 2012.

[9] M. Beard, S. Reuter, K. Granström, B.-T. Vo, B.-N. Vo, and A. Scheel
Multiple extended target tracking with labelled random finite sets
IEEE Trans. Signal Process., vol. 64, no. 7, pp. 1638–1653, Apr. 2016.

[10] A. Swain and D. Clark
The PHD filter for extended target tracking with estimable shape parameters of varying size
In *Proc. Int. Conf. Inf. Fusion*, Singapore, Jul. 2012, pp. 1111–1118.

[11] H. Raiffa and R. Schlaifer
Applied Statistical Decision Theory. Division of Research, Graduate School of Business Administration, Harvard University, Cambridge, MA, USA, 1961.

[12] B.-T. Vo and B.-N. Vo
Labeled random finite sets and multi-object conjugate priors
IEEE Trans. Signal Process., vol. 61, no. 13, pp. 3460–3475, Apr. 2013.

[13] J. Williams
Marginal multi-Bernoulli filters: RFS derivation of MHT, JIPDA, and association-based MeMBer
IEEE Trans. Aerosp. Electron. Syst., vol. 51, no. 3, pp. 1664–1687, Jul. 2015.

[14] A. F. Garcia-Fernandez, J. Williams, K. Granström, and L. Svensson
Poisson multi-Bernoulli mixture filter: Direct derivation and implementation
IEEE Trans. Aerosp. Electron. Syst., vol. 54, no. 4, pp. 1883–1901, Aug. 2018.

[15] Y. Xia, K. Granström, L. Svensson, and A. F. G. Fernández
Performance evaluation of multi-bernoulli conjugate priors for multi-target filtering
In *Proc. Int. Conf. Inf. Fusion*, Xi'an, China, Jul. 2017.

[16] S. Blackman and R. Popoli
Design and Analysis of Modern Tracking Systems. Norwood, MA, USA: Artech House, 1999.

[17] K. Granström, M. Fatemi, and L. Svensson
Gamma Gaussian inverse-Wishart Poisson multi-Bernoulli Filter for extended target tracking
In *Proc. Int. Conf. Inf. Fusion*, Heidelberg, Germany, Jul. 2016, pp. 893–900.

[18] K. Granström and U. Orguner
On spawning and combination of extended/group targets modeled with random matrices
IEEE Trans. Signal Process., vol. 61, no. 3, pp. 678–692, Feb. 2013.

[19] K. Granström, L. Svensson, S. Reuter, Y. Xia, and M. Fatemi
Likelihood-based data association for extended object tracking using sampling methods
IEEE Trans. Intell. Veh., vol. 3, no. 1, pp. 30–45, Mar. 2018.

[20] R. L. Graham, D. E. Knuth, and O. Patashnik
Concrete Mathematics. Reading, MA, USA: Addison–Wesley, 1988.

[21] M. Fatemi, K. Granström, L. Svensson, F. Ruiz, and L. Hammarstrand
Poisson multi-Bernoulli mapping using Gibbs sampling
IEEE Trans. Signal Process., vol. 65, no. 11, pp. 2814–2827, Jun. 2017.

[22] K. Engel
On the average rank of an element in a filter of the partition lattice
J. Combinatorial Theory, A, vol. 65, no. 1, pp. 67–78, 1994.

[23] E. R. Canfield
Engel's inequality for bell numbers
J. Combinatorial Theory, A, vol. 72, no. 1, pp. 184–187, 1995.

[24] Y. Bar-Shalom and W. D. Blair
Multitarget-Multisensor Tracking: Applications and Advances, vol. III. Norwood, MA, USA: Artech House, 2000.

[25] A. Scheel, K. Granström, D. Meissner, S. Reuter, and K. Dietmayer
Tracking and data segmentation using a GGIW filter with mixture clustering
In *Proc. Int. Conf. Inf. Fusion*, Salamanca, Spain, Jul. 2014.

[26] K. Murty
An algorithm for ranking all the assignments in order of increasing cost
Oper. Res., vol. 16, no. 3, pp. 682–687, 1968.

[27] K. Granström, S. Reuter, M. Fatemi, and L. Svensson
Pedestrian tracking using velodyne data—Stochastic optimization for extended object tracking
In *Proc. IEEE Intell. Veh. Symp.*, Redondo Beach, CA, USA, Jun. 2017, pp. 39–46.

[28] J. Williams
Graphical model approximations to the full Bayes random finite set filter
CoRR, vol. abs/1105.3298, 2011. [Online]. Available: http://arxiv.org/abs/1105.3298

[29] J. Williams
Hybrid Poisson and multi-Bernoulli filters
In *Proc. Int. Conf. Inf. Fusion*, Jul. 2012, pp. 1103–1110.

[30] J. Williams
An efficient, variational approximation of the best fitting multi-Bernoulli filter
IEEE Trans. Signal Process., vol. 63, no. 1, pp. 258–273, Jan. 2015.

[31] B.-T. Vo, B.-N. Vo, and D. Phung
Labeled random finite sets and the Bayes multi-target tracking filter
IEEE Trans. Signal Process., vol. 62, no. 24, pp. 6554–6567, Dec. 2014.

[32] W. Koch
Bayesian approach to extended object and cluster tracking using random matrices
IEEE Trans. Aerosp. Electron. Syst., vol. 44, no. 3, pp. 1042–1059, Jul. 2008.

[33] M. Feldmann, D. Fränken, and J. W. Koch
Tracking of extended objects and group targets using random matrices
IEEE Trans. Signal Process., vol. 59, no. 4, pp. 1409–1420, Apr. 2011.

[34] K. Granström, A. Natale, P. Braca, G. Ludeno, and F. Serafino
PHD extended target tracking using an incoherent X-band radar: Preliminary real-world experimental results
In *Proc. Int. Conf. Inf. Fusion*, Salamanca, Spain, Jul. 2014.

[35] K. Granström, A. Natale, P. Braca, G. Ludeno, and F. Serafino
Gamma gaussian inverse wishart probability hypothesis density for extended target tracking using x-band marine radar data
IEEE Trans. Geosci. Remote Sens., vol. 53, no. 12, pp. 6617–6631, Dec. 2015.

[36] M. Wieneke and W. Koch
A PMHT approach for extended objects and object groups
IEEE Trans. Aerosp. Electron. Syst., vol. 48, no. 3, pp. 2349–2370, Jul. 2012.

[37] S. Davey, M. Wieneke, and H. Vu
Histogram-PMHT unfettered
IEEE J. Sel. Topics Signal Process., vol. 7, no. 3, pp. 435–447, Jun. 2013.

[38] G. Vivone, P. Braca, K. Granström, and P. Willett
Multistatic Bayesian extended target tracking
IEEE Trans. Aerosp. Electron. Syst., vol. 52, no. 6, pp. 2626–2643, Dec. 2016.

[39] G. Vivone, P. Braca, K. Granström, A. Natale, and J. Chanussot
Converted measurements random matrix approach to extended target tracking using x-band marine radar data
In *Proc. Int. Conf. Inf. Fusion*, Washington, DC, USA, USA, Jul. 2015, pp. 976–983.

[40] G. Vivone, P. Braca, K. Granström, A. Natale, and J. Chanussot
Converted measurements bayesian extended target tracking applied to x-band marine radar data
J. Adv. Inf. Fusion, vol. 12, no. 2, pp. 189–210, Dec. 2017.

[41] M. Schuster, J. Reuter, and G. Wanielik
Probabilistic data association for tracking extended group targets under clutter using random matrices
In *Proc. Int. Conf. Inf. Fusion*, Washington, DC, USA, Jul. 2015, pp. 961–968.

[42] K. Granström and U. Orguner
Estimation and maintenance of measurement rates for multiple extended target tracking
In *Proc. Int. Conf. Inf. Fusion*, Singapore, Jul. 2012, pp. 2170–2176.

[43] U. Orguner
A variational measurement update for extended target tracking with random matrices
IEEE Trans. Signal Process., vol. 60, no. 7, pp. 3827–3834, Jul. 2012.

[44] K. Granström and U. Orguner
A new prediction update for extended target tracking with random matrices
IEEE Trans. Aerosp. Electron. Syst., vol. 50, no. 2, Apr. 2014.

[45] K. Granström and U. Orguner
On the reduction of Gaussian inverse wishart mixtures
In *Proc. Int. Conf. Inf. Fusion*, Singapore, Jul. 2012, pp. 2162–2169.

[46] M. Beard, B.-T. Vo, B.-N. Vo, and S. Arulampalam
Gaussian mixture PHD and CPHD filtering with partially uniform target birth
In *Proc. Int. Conf. Inf. Fusion*, Singapore, Jul. 2012, pp. 535–541.

[47] S. Yang, M. Baum, and K. Granström
Metric for performance evaluation of elliptic extended object tracking methods
In *Proc. IEEE Int. Conf. Multisensor Fusion Integr. Intell. Syst.*, Baden-Baden, Germany, Sep. 2016, pp. 523–528.

[48] C. R. Givens and R. M. Shortt
A class of Wasserstein metrics for probability distributions
Michigan Math. J., vol. 31, no. 2, pp. 231–240, 1984.

[49] A. S. Rahmathullah, A. F. García Fernández, and L. Svensson
Generalized optimal sub-pattern assignment metric
In *Proc. Int. Conf. Inf. Fusion*, Jul. 2017, pp. 1–8.

[50] D. Schuhmacher, B.-T. Vo, and B.-N. Vo
A consistent metric for performance evaluation of multi-object filters
IEEE Trans. Signal Process., vol. 56, no. 8, pp. 3447–3457, Aug. 2008.

Karl Granström (M'08) received the M.Sc. degree in applied physics and electrical engineering in May 2008, and the Ph.D. degree in automatic control in November 2012, both from Linköping University, Linkping, Sweden.

He is currently a Postdoctoral Research Fellow with the Department of Signals and Systems, Chalmers University of Technology, Gothenburg, Sweden. He previously held Postdoctoral positions with the Department of Electrical and Computer Engineering, University of Connecticut, USA, from September 2014 to August 2015, and with the Department of Electrical Engineering, Linköping University, from December 2012 to August 2014. His research interests include estimation theory, multiple model estimation, sensor fusion and target tracking, especially for extended targets.

Dr. Granström was recipient of paper awards at the Fusion 2011 and Fusion 2012 conferences. In 2018, the International Society of Information Fusion (ISIF) awarded him the ISIF Young Investigator Award for his contributions to extended object tracking and his service to the research community.

Maryam Fatemi received the M.Sc. degree in communication systems engineering from AmirKabir University of Technology, Tehran, Iran, in 2008, and the Ph.D. degree in electrical engineering from Chalmers University of Technology, Gothenburg, Sweden in 2016.

In November 2016, she joined Autoliv Sverige AB and currently she is with Zenuity, Gothenburg, Sweden. Her research interests include Bayesian Inference and nonlinear filtering with applications to sensor data fusion, autonomous driving and active safety systems.

Lennart Svensson was born in Älvängen, Sweden, in 1976. He received the M.S. degree in electrical engineering in 1999 and the Ph.D. degree in signal processing, in 2004, both from Chalmers University of Technology, Gothenburg, Sweden.

He is currently Professor of signal processing with the Chalmers University of Technology. His main research interests include machine learning and Bayesian inference in general, and nonlinear filtering and tracking in particular.